

THE EFFECT OF PROGESTIN ON MAMMARY GLAND BRANCHING
MORPHOGENESIS IN VITRO

By

Gabriele M. Meyer

A DISSERTATION

Submitted to
Michigan State University
in partial fulfillment of the requirements
for the degree of

DOCTOR OF PHILOSOPHY

Genetics

2011

ABSTRACT

THE EFFECT OF PROGESTIN ON MAMMARY GLAND BRANCHING MORPHOGENESIS IN VITRO

By

Gabriele M. Meyer

Mouse mammary organoids that express progesterone receptor A (PRA) produce tubules in response to hepatocyte growth factor (HGF) when cultured in collagen gels. These structures resemble ducts in the mouse mammary gland. When treated with the combination of HGF and the synthetic progestin, promogestone (R5020), tubulogenesis is stunted to form shorter tubules that resemble sidebranches in early pregnancy. It was hypothesized that R5020 reduces early HGF/cMet signaling to produce sidebranch-like tubules. Therefore, the HGF-induced pathway controlling early extension formation was determined and how R5020 altered HGF/cMet signaling was analyzed. Using molecular inhibitors and shRNA, it was found that HGF activates Rac1 to form extensions in the first step of tubulogenesis and that Rac1 activity is Src and FAK dependent. In addition, it was discovered that R5020 increases extracellular laminin to reduce the Src, FAK and Rac1 pathway leading to reduced extensions. This is likely mediated through PRA, as PRA is the predominant PR isoform expressed in organoids. This may in part explain blunted tubulogenesis observed with combined HGF and R5020 treatment and further supports a role for PRA in sidebranching during pregnancy.

DEDICATION

To my father Bill, mother Carolyn, and my sisters and brothers Karen, Bill, Stephanie, David and Nicholas. I could not have done all this without you.

ACKNOWLEDGEMENTS

I would like to thank my mentor, Dr. Sandra Haslam, for support and guidance on my project and graduate school. Thanks to members of my committee, Dr. Susan Conrad, Dr. Michele Fluck, Dr. Richard Miksicek, Dr. Chengfeng Yang for additional guidance on my project. In addition, thanks to Dr. Miksicek on help and feedback with the design of PRAKO and PRBKO mice, and Dr. Yang for his advice on the mouse mammary organoid project. Thanks to Dr. Bruce Uhal for his guidance on my committee during my comprehensive and oral exams. Thanks to Jeff Leipprandt, Jianwei Xie and other members of the Haslam Lab (past and present) who helped me with my project. Thanks to Dr. Rich Schwartz, Dr. John Fyfe, Dr. Karen Frederici, Dr. Karl Olsen and members of the Breast Cancer Signaling Network consortium for advice and technical assistance. Thanks to Dr. Thomas Saunders, Elizabeth Hughes and the University of Michigan Transgenic Animal Model Core Facility for assistance with the PRAKO and PRBKO mice. Thanks to staff of the University Laboratory Animal Resources for assistance with mouse breeding. Thanks to Dr. Andrea Almalfitano, Sarah Roosa and members of the Almalfitano Lab for assistance on generating adenovirus. Finally thanks to the support of all my friends and family.

TABLE OF CONTENTS

LIST OF TABLES	vi
LIST OF FIGURES	vii
LIST OF ABBREVIATIONS	ix
CHAPTER 1	
LITERATURE REVIEW	1
CHAPTER 2	
MATERIALS AND METHODS	9
CHAPTER 3	
RESULTS	16
CHAPTER 4	
DISCUSSION	23
APPENDICES	
APPENDIX A, Progesterone Receptor Isoform Knockouts	30
APPENDIX B, Figures	35
REFERENCES	67

LIST OF TABLES

TABLE 1	
Quantitative RT-PCR analysis of fold change of Laminin- γ 2 mRNA after knockdown with Lm γ 2 shRNA	66

LIST OF FIGURES

FIGURE 1	Tubulogenesis of mammary organoids	35
FIGURE 2	Time course of morphological changes induced by HGF.....	36
FIGURE 3	The effect of Rho and Rac1 inhibition on HGF-induced tubulogenesis	37
FIGURE 4	Rac1 inhibition reduces HGF-induced tubulogenesis	38
FIGURE 5	Rac1 shRNA blocks HGF-induced tubulogenesis	40
FIGURE 6	Src inhibition blocks HGF-induced tubulogenesis	42
FIGURE 7	FAK inhibition blocks HGF-induced tubulogenesis	44
FIGURE 8	The effect of MEK inhibition on HGF induced tubulogenesis	46
FIGURE 9	The effect of PI3K inhibition on HGF-induced tubulogenesis	48
FIGURE 10	R5020 reduces HGF-induced tubulogenesis	50
FIGURE 11	The effects of collagen I vs. laminin on HGF-induced tubulogenesis	52
FIGURE 12	R5020 induces Laminin- γ 2 expression in mammary organoids	53
FIGURE 13	Laminin- γ 2 shRNA reverses the effect of HGF+R5020 response in organoids	55
FIGURE 14	The effect of a neutralizing antibody against α 6-integrin on the HGF+R5020 response in organoids	57

FIGURE 15	
Proposed mechanism for R5020-blunted tubulogenesis	59
FIGURE 16	
Strategy for developing PRA and PRB knockout Balb/c mice	61
FIGURE 17	
Identification of PRAKO and PRABKO alleles in ES cells	63
FIGURE 18	
Identification of germline PRBKO allele	64
FIGURE 19	
Timeline for generating PRAKO and PRBKO mice	65

LIST OF ABBREVIATIONS

Amphiregulin (AREG)

Basal media (BM)

Collagen (Col)

Estrogen (E)

Epidermal growth factor (EGF)

Estrogen receptor (ER)

Extracellular matrix (ECM)

Fibroblast growth factor (FGF)

Focal adhesion kinase (FAK)

FAK inhibitor-14 (FAK-i14)

Growth factors (GF)

Hepatocyte growth factor (HGF)

Laminin (Lm)

Luminal epithelial cell (LEC)

Madine Darby canine kidney cells (MDCKs)

Map kinase inhibitor (U0126)

Myoepithelial cell (MEC)

Phosphoinositide-3 kinase (PI3K)

PI3K inhibitor (LY294002)

Progesterone/progestin (P)

Progesterone receptor (PR)

Progesterone receptor A (PRA)

Progesterone receptor B (PRB)

PRA knockout (PRAKO)

PRB knockout (PRBKO)

Promogestone (R5020)

Rac1 inhibitor (NSC23766)

Rho kinase inhibitor (Y-27632)

Terminal end bud (TEB)

Transforming growth factor (TGF)

Src kinase inhibitor (PP2)

CHAPTER 1

LITERATURE REVIEW

Overview

In the mouse mammary gland, estrogen (E) and progesterone (P) regulate the epithelium and stroma to influence ductal elongation, sidebranching and alveologensis. From puberty to sexual maturity, E stimulates growth factor (GF) production from stromal cells and epithelial cells (1-4). GFs, in turn, act on the epithelium leading to ductal elongation and branching until the ducts have reached the limits of the fat pad (5-7). In pregnancy, increases in E and P are concurrent with sidebranching and alveologensis. Although E is present, P is responsible for the formation of sidebranches and alveoli (8). It is likely that crosstalk between E-dependant GFs and P promotes sidebranching and alveologensis. However, this interaction is not well understood. Complicating this issue is that there are conflicting reports about the function of progesterone receptor isoforms PRA and PRB in sidebranching.

In order to understand specific P and GF interactions, cell culture systems have been useful. However, care must be taken when interpreting information from monolayer culture as it does not represent the three-dimensional (3D) architecture of the gland. Cell signaling is likely altered in such cases. To address this problem, cells cultured in 3D extracellular matrices are used. In collagen gel culture, the mesenchymal factor hepatocyte growth factor (HGF) causes tubule formation in primary mammary epithelial organoids (3, 9, 10). These structures resemble mammary ducts observed *in vivo*. The synthetic progestin promogestone (R5020) stunts HGF-induced tubulogenesis to cause shorter tubes that resemble sidebranches (10). This response is mediated through PRA in organoids from virgin adult mice (11) and is inhibited by the PR

antagonist RU486 (10). The mechanism of R5020-mediated blunting of tubulogenesis might mimic a potential mechanism of sidebranching during early pregnancy. Therefore the aim of this research is to understand the mechanism of action of P/PRA on tubule blunting and to determine how P/PRA signaling influences HGF signaling to cause sidebranches in vitro.

Mouse mammary gland composition

The architecture of the mammary gland and the distribution of hormone receptors highlight the complexity of crosstalk controlling development. In the epithelial component, an inner layer of luminal epithelial cells (LECs) line the lumen of ducts while basal myoepithelial cells (MECs) surround the LECs (12). Only a subset of the LECs are estrogen receptor (ER) and progesterone receptor (PR) positive (2, 13, 14). Most proliferation occurs in hormone receptor negative cells, indicating that paracrine signaling is responsible for hormone-induced proliferation and differentiation of the gland (13-16).

A specialized extracellular matrix (ECM) rich in collagen, laminin and fibronectin separates the epithelium from the stromal compartment of the gland. Both epithelial cells and stromal cells deposit this basement membrane (17) and the composition is developmentally regulated (18, 19). The role of the ECM is to regulate cellular organization and polarity supporting integrity of the gland, and to regulate epithelial responsiveness to hormones (20, 21). Regulation of the epithelium by the ECM may be through autocrine and paracrine mechanisms and is mediated by integrins expressed on the surface of cells. In the mammary gland, the composition of the ECM may be structure dependent. It has been noted that collagen I is concentrated near the large main ducts while laminin expression appears near shorter branches and alveoli (18). This implicates specific ECMs in directing the formation of distinct mammary structures.

Finally, in the stroma, ER-positive cells produce essential growth factors necessary for epithelium development (1, 3, 22). Any disruption between the epithelium, stroma and basement membrane results in impaired mammary gland organogenesis, highlighting the importance of the microenvironment in development of the gland.

Hormonal and Growth Factor influence on mouse mammary gland development in vivo

Ductal elongation and branching: the role of E/ER and HGF/cMet

At birth a rudimentary ductal system exists that grows minimally until the animal reaches puberty. Despite the presence of hormone receptors the gland is non-responsive to steroid hormones prior to puberty (23). At about 3-4 wks of age, with the onset of estrus cycles, E stimulates ductal development. Terminal end buds (TEBs) develop and proliferate to elongate the ducts. Ductal elongation and branching continues with each estrous cycle until the mouse reaches sexual maturity. At this point, the ducts have reached the limits of the mammary fat pad. It is known that E signaling through ER α is primarily responsible for this process (2).

Studies have indicated that E action on the epithelium is both direct and indirect (1, 2). E stimulates both the epithelium and neighboring stromal cells to produce a number of GFs that act on the epithelium to promote ductal elongation and branching. Epidermal growth factor (EGF), amphiregulin (AREG), fibroblast growth factor (FGF), and transforming growth factor TGF β have all been identified as factors affecting proliferation and morphogenesis during ductal development (6, 24-27).

Yet another E-dependent stroma-derived growth factor implicated in ductal branching is HGF (5, 28-31). HGF action in the epithelium is mediated through the tyrosine kinase receptor, cMet. When HGF binds, cMet activates a number of downstream pathways that affect proliferation, cell survival, and motility (32). Expression of HGF and cMet during development

is coordinated. From puberty to sexual maturity, levels of HGF increase in the stroma while cMet levels increase in the epithelium (33). This is concurrent with ductal elongation and branching of the ducts. Recent evidence from mammary specific ablation of cMet suggests that HGF/cMet signaling is important for secondary branching off of main ducts during development (5). The role of cMet in the mammary gland during pregnancy was not reported for these mice. However, during pregnancy, expression of HGF and cMet decline and expression is absent during late pregnancy and lactation (33). This suggests that the HGF/cMet role in alveologenesis and lactation is less important. Yet, a role in sidebranch formation during early pregnancy cannot be dismissed.

Sidebranching: the role of P/PR

In the fully mature virgin gland and during pregnancy, E and P promote the second phase of development, sidebranching and alveologenesis (34). Short branches form laterally off ducts, and expand to form alveoli. During this time the level of estrogen receptor (ER) declines while the level of progesterone receptor (PR) increases (35, 36) indicating that P/PR signaling is a major contributor to this stage.

PR exists as two isoforms, PRA and PRB. The receptors are encoded within a single gene under the control of two different promoters (37, 38). PRA and PRB are nearly identical with the exception that PRB has an additional 164 amino acids at the N-terminus (37-39). The receptor may follow a classical nuclear receptor signaling pathway to activate gene transcription (40). Information from cell lines suggest that PRB is a strong activator of transcription while PRA has a repressing function (40-43). Additionally, PR may activate non-genomic pathways through interactions with Src in the cytoplasm (44-46).

The two isoforms function differently in mouse mammary gland development. Knockout studies have shown that PRB is important for sidebranching and alveologenesis but that PRA is non-essential(8, 47). However, it should be noted that the PR-isoform knockouts were in a mixed genetic background of C57/black x 129SV, and that the genetic background of a mouse dictates hormonal response. It was reported that adult C57/black mice have a reduced response to P compared to the Balb/c strain of mice (48) and developmental studies in Balb/c mice suggest that the role of PRA in mammary gland development might have been overlooked. Only PRA is expressed in the gland in the virgin mouse during ductal development (14). In addition PRA is the only isoform detected in early pregnancy, as sidebranches begin to appear (14). PRB is detected later in pregnancy with the onset of alveologenesis (14). Furthermore, sidebranch formation can be induced in ovariectomized virgin adult mice treated with P alone (49). Taken together, this suggests that P signaling through PRA can promote sidebranching while PRB is responsible for alveologenesis.

In vitro model of mammary gland branching

The mammary gland can be modeled in vitro by placing primary mammary epithelial organoids in a 3 dimensional matrix. This can then become a platform for analyzing the interaction between hormone and GF signaling. When primary organoids containing LECs and MECs are placed in collagen gels and treated with HGF, the cells are able to form tubes (3, 10). These tubules resemble ductal structures in the mouse prior to pregnancy. Interestingly, the process of HGF-induced tubulogenesis can be modified with the inclusion of a synthetic progestin, promogestone (R5020). This results in shorter tubules resembling sidebranches in the pregnant mouse (10, 11). The combination of both HGF and R5020 is needed for this effect, as R5020 alone promotes only lumen formation (10). Furthermore, R5020 blunting of HGF-

induced tubulogenesis was blocked by RU486, a PR-specific inhibitor (10) indicating that this is a PR-specific signaling event. Analysis of PR isoform expression revealed that PRA is the predominant isoform expressed in organoids (11). Therefore R5020 blunting of tubulogenesis is likely mediated through PRA. The HGF signaling pathway(s) regulating tubule formation and morphology in organoids is not known. Nor is the effect of R5020 on the morphology pathway known. However, information from other tubulogenesis models can help identify potential signaling mechanisms.

Tubulogenesis has been observed for other epithelial cells including those from kidney, lung and salivary gland (50-52). Key information about tubulogenesis has been obtained from Madine Darby canine kidney cells (MDCK; (53, 54). After HGF stimulation, epithelial cells send out cytoplasmic extensions into the surrounding matrix. A single layer chain of cells invades further, lengthening the growing tube. Following this period of tubule development, the epithelial cells undergo a re-differentiation stage where they form bi-layered cords of cells and finally mature tubules with complete lumens (54). This same sequence of events has also been observed for HGF-treated mammary organoids (11). However, mainly LECs produce extensions to lead tubulogenesis, while MECs follow (11).

Tubule length is determined by the distance epithelial cells migrate from the body of the organoid, and this depends on changes in actin polymerization. Members of the Rho family GTPases, Rac1 and Rho, regulate actin dynamics. Rac1 contributes to actin protrusions at the leading edge of migrating cells and is implicated in extension and chain formation during tubulogenesis (55-59). Rho controls the formation of stress fibers and focal adhesions at the rear of migrating cells (55, 56). Rho contributes to later stages of tubule development leading to mature tubules (57, 60). A number of critical pathways acting upstream of Rac1 and Rho for

tubulogenesis and cell migration have been identified including MAP kinase (MAPK; (54)), phosphoinositide-3 kinase (PI3K; (60, 61), Src kinase (62, 63), and focal adhesion kinase (FAK; (58). Though the signaling pathways driving mammary organoid tubulogenesis are not known, those established in MDCK cells may also be relevant. Because R5020/PR signaling was shown to blunt HGF-induced tubulogenesis in PRA-expressing mammary organoids (10, 11) it was hypothesized that R5020 signaling through PRA reduced Rac1-GTP activity to inhibit extension formation and blunt HGF-induced tubulogenesis. Therefore, the goal of this project was (1) to determine the HGF-induced signaling pathway responsible for early morphological events during tubulogenesis, (2) to determine the effects of R5020 on that pathway, (3) to determine the mechanism of how R5020 alters the morphological pathway and (4) to generate PRA and PRB knockout mice in Balb/c background to confirm the role of PRA in sidebranching in vitro and in vivo.

CHAPTER 2

MATERIALS AND METHODS

Animals

Balb/c virgin adult females (16-24 week old) from our colony were used as the source of mammary gland tissue for primary cell culture. Animal use was in accordance with accepted standards of humane animal care, and approved by the All University Committee on Animal Use and Care at Michigan State University.

Cell Culture

Collagen gel 3-D Culture

For 3D collagen cultures, primary mouse mammary epithelial organoids were isolated as previously published (11). Prior to plating cells, 96-well or 24-well culture plates were first coated with an underlay of 40 μ L/well or 250 μ L/well, of neutralized rat tail collagen I (2 mg/ml, BD Biosciences, Bedford, MA). For 96-well culture plates, the isolated organoids were suspended in 2 mg/ml neutralized collagen I and plated at a density of 1×10^5 cells/well and a total volume of 75 μ L/well. For 24-well culture plates, organoids were suspended in the same concentration of collagen but plated at a density of 1.4×10^6 cells/well and a total volume of 600 μ L/well. The cell/collagen suspensions were allowed to set for 30 minutes at 37°C before addition of media. Treatments were done in triplicates for 96-well culture plates, and in quadruplicates for 24-well culture plates. Cultures were maintained in serum-free medium with or without HGF or progesterin (basal medium: serum- and phenol red-free DMEM/F12 (Sigma, St. Louis, MO), supplemented with 100 ng/ml human recombinant insulin, 1 mg/ml fatty acid-free

BSA (fraction V), 100 µg/ml penicillin, and 50 µg/ml streptomycin. Treatments included 50 ng/ml HGF, (Sigma, St. Louis, MO), and 20 nM of the synthetic progestin, R5020, (Perkin Elmer, Boston, MA) that were added at the time of plating. Organoid cultures were maintained in 5% CO₂ at 37°C for up to 3 days and culture media was replaced every 48h.

For all inhibitor studies, 100 µM Rac1 inhibitor NSC23766 (Tocris Bioscience, Ellisville, MO), 50 µM Rho kinase inhibitor Y27632 (Tocris Bioscience), 10 µM FAK inhibitor-14 (Tocris Bioscience), 10 µM PI3K inhibitor LY294002 (Cell Signaling Technology, Danvers, MA), 10 µM MEK inhibitor U0126 (Cell Signaling Technology), or 20 µM Src inhibitor PP2 (Cell Signaling Technology) were added to the cell/collagen suspensions prior to plating as well as included in media to maintain a constant concentration. Cell viability was assessed after 24h and 48h of treatment. Organoids were labeled with Alexa Fluor 555 conjugated annexin V (Invitrogen, Carlsbad, CA) as per manufacturer's recommendation and cell viability was assessed using a Nikon inverted epifluorescence scope (Mager Scientific, Dexter, MI).

Matrigel 3-D culture

Freshly isolated organoids were resuspended in growth factor reduced Matrigel (BD Biosciences, Bedford, MA) and plated at a density of 1×10^5 cells/well in a 96-well plate. The cell/Matrigel suspensions were allowed to set for 30 minutes at 37°C before addition of media. Treatments were done in triplicates for 96-well culture plates. Treatments included BM, HGF, R5020 or HGF+R5020 at the concentration indicated above that were added at the time of plating. Organoid cultures were maintained in 5% CO₂ at 37°C for up to 7 days and culture media was replaced every 48h.

Monolayer Cell Culture

6-well plates were precoated with 50 µg/mL of collagen I or laminin-1 (BD Biosciences, Bedford, MA) prior to plating of cells. Isolated primary mammary epithelial organoids were plated as monolayer with 4×10^6 cells/well and cultured in BM for 48h to allow attachment of the cells to the different ECMs. After 48h, media was replaced with fresh BM or BM containing HGF. Cultures were then harvested after 4h of treatment using the Rac1 lysis buffer. The supernatants were used for Rac1-GTP assay as outlined below.

Adenovirus Vector and Virus production

shRNA sequences targeting mouse Rac1, Laminin-5 (γ -2 subunit) and scramble sequences were designed using shRNA ExplorerTM program (Gene Link, Hawthorne, NY). Design included 5' Bgl II and 3' Cla I overhangs that allowed subcloning into pSuper[®] vector (Oligoengine, Seattle, WA; gift from Dr. Amalfitano) and placed the shRNA sequences under the control of a pol II H1-promoter. The resulting H1-shRNAs were subsequently removed from pSuper[®] with Sal I and BamH I restriction enzymes and placed within pShuttle-IRES-hrGFP[®] vector (Agilent Technologies, Santa Clara, CA; gift from Dr. Miranti) creating an H1-shRNA-CMV-GFP vector. This was linearized using Pme I and recombined with pAdEasy[®] (Agilent Technologies - Gift from Dr. Amalfitano) in BJ-5183 bacterial cells. Adenovirus was produced and purified as described in Luo et al., (64). Briefly, the adenovirus vectors were used to transfect HEK293 cells. After several serial passages in HEK293 cells, amplified virus was purified by sequential CsCl₂ gradient centrifugations. The purified virus was dialyzed against 10mM Tris (pH 8.0) and stored at -80°C in 1% sucrose, 1x PBS until use. The tissue culture infectious doses (TCID₅₀) were in a range of 10^9 - 10^{11} infectious particles/ml.

Knockdown of proteins by adenovirally delivered shRNA

Freshly isolated organoids were infected in suspension in BM with adenovirus (MOI 50) carrying GFP-vector, shRNA vectors, or scramble vector with gentle agitation for 3.5h at 37°C. The infected organoids were centrifuged at 200 x g for 5 min. and the viral supernatant was removed. Organoids were then washed with 1xHBSS, and resuspended in basal media (BM). Total cell numbers were determined by Crystal Violet staining as previously described (11) and viability was analyzed by Trypan Blue exclusion. Organoids were plated in collagen gel as described before and maintained in BM prior to treatment. To determine infectivity, GFP expression was analyzed using a Nikon inverted epifluorescence scope (Mager Scientific, Dexter, MI) 24h post infection. 80-90% infection was obtained. Cell viability was assessed 24h and 48h after infection by annexin V labeling as was described above. For Rac1 knockdown, cultures were cultured in BM at for 48h to achieve knockdown of proteins, as analyzed by immunoblotting. For Laminin- γ 2 (Lm γ 2) knockdown, organoids were maintained in BM for 24h and knockdown was analyzed by quantitative RT-PCR. Following knockdown, cultures were treated with BM, HGF or the combination of HGF and R5020. Cultures were maintained for 3 days changing the media after 48h as before.

Morphometrics

Images of primary mammary organoids were captured with a 20x lens using a Nikon TMS-F inverted scope (Nikon, Melville, NY) equipped with a Q imaging Micropublishing 5.0 RTV camera and Qcapture pro software (QImaging Corporation, Surrey, B.C., Canada). Images were analyzed for extension and tubule number per organoid with ImageJ software (National Institutes of Health, Bethesda, MD). The width and length of projections from the organoid body were used to classify structures into extensions, chains and tubes. In the α 6-integrin blocking

antibody experiments, structures longer than the average tubule length (≥ 140 pixels) were considered long tubules. For shRNA cultures, images of organoids expressing 80-90% GFP were captured using a Nikon inverted epifluorescence scope with 10x lens (Mager Scientific, Dexter, MI) and analyzed with MetaMorph software. Quantitation of extension and tubule number per organoid was determined from 45 or more organoids per treatment from three or more separate experiments. For Lm γ 2shRNA experiments, structures longer than the average tubule length (≥ 50 pixels) were considered long tubules. The results are reported as the mean \pm SEM, and differences are significant at $P < 0.05$ with ANVOA.

Rac1-GTP assay

Rac1-GTP assays were performed following a modified method from Yamazaki et al., 2009. Collagen gels containing organoids were homogenized in Rac1 lysis buffer (50mM Tris pH 7.5, 150mM NaCl, 5mM MgCl₂, 1% NonidetP-40, 0.5% deoxycholate, 1mM Na₃VO₄, 0.1% SDS, protease inhibitor cocktail; Sigma, St. Louis, MO). Lysates were cleared by centrifugation and the protein supernatant was reserved. Small aliquots of the supernatants were set aside for total Rac1 and Erk 1/2 immunoblots. The remaining supernatants were used for Rac1 pull down assays using PAK-PBD protein agarose beads (Cytoskeleton, Denver, CO) as per manufacturer's recommendation. Beads were washed in 1 x PBS and resuspended in NuPAGE Sample Reducing Agent and Loading dye (Invitrogen, Carlsbad, CA) then heated for 10 min at 70°C. Denatured beads and proteins were separated on a 4-12% Bis-Tris NuPAGE gel (Invitrogen) then transferred to a nitrocellulose membrane (Schleicher & Schuell, Keene, NH). The membrane was blocked in Odyssey Blocking Buffer (Li-Cor Biosciences, Lincoln, NB) diluted in 1 x TTBS (1:1), and incubated overnight in anti-Rac1, clone 23A8 antibody (Millipore, Billerica, MA, 1:1000 dilution), and anti-Erk 1/2 antibody (Santa Cruz Biotechnology, Santa Cruz, CA, 1:1000

dilution) for a loading control. Membranes were washed with 1 x TTBS and incubated for 1h with 1:5000 dilutions of IRDye® 680 or IRDye® 800 secondary antibodies against mouse or rabbit (Licor Biosciences). Membranes were scanned using an Odessey scanner (Licor Biosciences) and densitometric measurements of protein bands were assessed using ImageJ (National Institutes of Health, Bethesda, MD) to determine the ratio of Rac1-GTP to total Rac1. Since actin levels changed with treatments and Erk1/2 did not change, Erk1/2 level was used as a loading control.

Immunoblotting

Protein supernatants were prepared as outlined above and were directly used for western blotting of total and phosphorylated proteins using the following antibodies: pAKT 1/2/3 (Ser 473, 1:200 dilution), PI3 Kinase p85 α (B9, 1:500 dilution), pErk (E-4, 1:200 dilution), Erk 1 (C-16, 1:1000 dilution), Laminin γ -2 (Lm γ 2; c-20, 1:200 dilution) and FAK (A-17, 1:1000 dilution) from Santa Cruz Biotechnology, Santa Cruz, CA. The pFAK (pY397, 1:1000 dilution) antibody was from Invitrogen (Carlsbad, CA). The pSrc (Y416, 1:200 dilution) and Src (1:1000 dilution) antibodies were obtained from Cell Signaling Biotechnology (Danvers, MA). For phospho-FAK, p-Tyr proteins were immunoprecipitated using pTyr antibody (PY99, Santa Cruz Biotechnology, Santa Cruz, CA) and an immunoblot was performed to detect pFAK. Erk1/2 was used as a loading control for all immunoblots. IRDye® 680 or IRDye® 800 secondary antibodies against mouse, rabbit or goat were used at 1:5000 dilutions. Erk1/2 level was used as a loading control and protein levels were normalized to Erk 1/2.

Antibody labeling

The procedure for antibody labeling of organoids in collagen gels was previously described (Haslam et al., 2008). Briefly, gels containing organoids were washed with PBS+

(PBS, 1 mM CaCl₂, 0.5 mM MgCl₂; pH 7.2). Gels were fixed in 4% paraformaldehyde in PBS+ and permeabilized with P buffer (PBS+, 0.025% saponin). Gels were then quenched with Q buffer (PBS+, 75 mM NH₄Cl, 20 mM glycine) and blocked 10 min in B buffer (PBS+, 0.025% saponin, 0.3% gelatin). Gels were incubated overnight at 4°C with the goat polyclonal Lmγ2 antibody and a mouse monoclonal antibody against cytokeratin-18 (K18; ab668-100-Abcam, Cambridge, MA) diluted 1:200 in B buffer. Gels were washed with P buffer and incubated for 1h with rabbit-anti-goat biotin (Dako, Denmark) diluted 1:400 in B buffer. Gels were rinsed with PBS+ and incubated overnight at 4°C with goat-anti-mouse Alexa 488 and streptavidin-Alexa 546 (Molecular Probes, Eugene, OR) diluted 1:200 in B buffer. Samples were washed P buffer then post-fixed in 4% paraformaldehyde in 0.1 M sodium cacodylate buffer (pH 7.2) and mounted to slides with fluorescence mounting media. A Pascal laser scanning confocal microscope (Carl Zeiss Inc., Thornwood, NY) was used to capture images. A 3-D Z plane series with a step size of 4 μM was used to generate each image.

RT-PCR

For RT-PCR of Lmγ2, organoids were infected and maintained in BM for 24h, then treated with HGF or HGF+R5020. 24h later, gels were removed and RNA was extracted using the Trizol method, described previously (65). cDNA was prepared from isolated RNA using random hexamer primers from RT² First Strand Kit (Qiagen, Valencia, CA) per manufacturer's instructions. A 7500 FAST RT-PCR System (Applied Biosystems, Carlsbad, CA) was used for RT-PCR. Gene expression assays were performed in triplicate with RT² SYBR Green ROX qPCR Mastermix (Qiagen) and prevalidated primers for Lmγ2 (LAMC2) and GAPDH. The

expression values were normalized to GAPDH and the Comparative Ct Method was used to determine the change in gene expression.

Blocking antibody cultures

Isolated primary organoids were pretreated in BM suspension with 10 µg/mL of GoH3 or IgG2a Isotype control (Becton-Dickinson, Franklin Lakes, NJ) for 30 min. Organoids were plated in collagen I containing 10 µg/mL GoH3 or IgG2a, and allowed to gel for 20 min prior to addition of HGF or HGF+R5020. Organoids were maintained as described above.

Statistical Analysis

All experiments were repeated up to 8 times. Values are presented as mean \pm S.E.M. Statistical significance was determined by Student's t-Test or ANOVA using SYSTAT (SYSTAT Software Inc., Chicago, IL) as appropriate and results considered significant at $p < 0.05$.

CHAPTER 3

RESULTS

HGF induces extensions to initiate tubulogenesis in mammary organoids by Rac1 activation

It was previously reported that organoids treated with HGF form duct-like tubules by 72h and that the addition of R5020 blunts tubule formation (10). As was described, LECs produce extensions that lead to tubulogenesis (11). The extensions progress to form chains of cells, cords and mature tubules (FIGURE 1). The blunting of tubulogenesis is hypothesized to be relevant to the mechanism through which progesterone promotes sidebranch development. It is not known when the blunting effect of R5020 occurs in the development of tubules. Therefore, as a first step, a time course of HGF-induced tubulogenesis was analyzed in organoids from 0-24h (FIGURE 2 A-B). When first plated, organoids have a rounded morphology. By 4h, HGF increased the number of cytoplasmic extensions. By 24h, chains and tubules were observed in HGF-treated organoids.

The pathway responsible for initiating tubulogenesis in organoids is not known and identifying this pathway can define where R5020 might act to blunt the HGF response. Rho GTPases Rac1 and Rho have been reported to regulate cell morphology in the MDCK model of tubulogenesis (57). To determine the roles of Rac1 and Rho in mammary organoid tubulogenesis, organoids were treated for 24h with HGF in the presence of the Rho kinase (ROCK) inhibitor, Y-27632, or the Rac1 inhibitor, NSC23766 (FIGURE 3 A). By 24h, ROCK inhibition did not prevent the formation of extensions or chains in HGF-treated organoids. After 48h, mature tubules were unable to form and migrating cells pinched off the organoid body (data not shown).

Similar results have been published for MDCK cells treated with Y-27632 (60). This suggests that Rho signaling regulates tubule maturation, the second stage of tubulogenesis. In contrast, Rac1 inhibition significantly reduced HGF-induced formation of chains and tubules by 24h (FIGURE 3 A, FIGURE 4 B). This suggests that Rac1 activity promotes extension and chain formation in the early steps of tubulogenesis. Consistent with this observation, HGF significantly increased levels of Rac1-GTP at 4h (FIGURE 3 B) when extensions were first observed. Though 24h treatment with the Rac1 inhibitor dramatically reduced chains and tubules, 4h treatment did not reduce extension number or Rac1-GTP (FIGURE 4 A-C). This indicates that a longer exposure time to the inhibitor was necessary to block tubulogenesis.

The observation that HGF increased Rac1-GTP during extension formation indicated that Rac1 could contribute to extension formation. As an alternative method to the Rac1-GTP inhibitor, Rac1 was silenced in organoids with shRNA to determine the role of Rac1 in extension formation. Two separate adenoviruses were created that contained a CMV-GFP cassette and shRNA against Rac1. The presence of GFP (GFP+) allowed infected and shRNA-producing cells to be differentiated from non-infected cells (GFP-). 48h after infection, organoids were treated with BM or HGF for 4h. Total Rac1 levels were assessed after 4h treatment and GFP+ extensions, chains and tubules were measured over 24h (FIGURE 5 A-C). Organoids infected with vector alone or scramble shRNA were able to make GFP+ and GFP- extensions, chains and tubules. The only extensions, chains and tubules that were able to form in shRNA treated organoids were GFP-. The absence of GFP indicated that cells in these structures were uninfected and thus not likely to contain Rac1 shRNA. There were virtually no GFP+ extensions in the shRNA treated organoids at 4h. By 24h, the number of GFP+ extension, chains and tubules were significantly reduced by 24h. Western blot confirmed that total Rac1 was reduced

by shRNAs (FIGURE 5 C). Taken together, these data confirmed a role for Rac1 in extension, and chain formation during HGF-induced tubulogenesis.

HGF-induced Rac1-GTP in mammary organoids is Src and FAK dependant

Src, FAK, PI3K, and MapK have all been reported to regulate Rac1, tubulogenesis and cell migration in other models (54, 58, 60-63, 66). Therefore, molecular inhibitors targeting Src, FAK, PI3K or MEK signaling were used to determine the regulator(s) of HGF-induced Rac1 in organoids. When organoids were treated with HGF in the presence of the Src inhibitor (PP2), extensions were significantly reduced compared to HGF-controls (FIGURE 6 A-B). By 24h, the Src inhibitor significantly reduced the number of chains and tubules. Furthermore, Src inhibition significantly reduced the level of Rac1-GTP at 4h compared to the HGF-control (FIGURE 6 C). This indicates that Src signaling downstream of HGF/cMet regulates Rac1 activity and extension formation in organoids. Similar results were observed with the FAK inhibitor (FAK inhibitor-14). After 4h, FAK inhibition significantly reduced extension formation (FIGURE 7 A-B). Chains and tubules were also significantly inhibited after 24h. In addition, FAK inhibition significantly reduced the level of Rac1-GTP compared to the HGF control (FIGURE 7 C). However, phosphorylated FAK levels were too low to be detected by immunoblot to confirm inhibition. In contrast to Src and FAK inhibition, when organoids were treated with HGF in the presence of the MEK inhibitor (U0126; FIGURE 8 A-C) or the PI3K inhibitor (LY294002; FIGURE 9 A-C) there was no significant inhibition of extensions and chains by 4 and 24h. In addition, the MEK and PI3K inhibitors did not significantly reduce the level of Rac1-GTP. The MEK inhibitor did reduce tubule formation by 60% (FIGURE 8 A-B) whereas the PI3K inhibitor did not (FIGURE 9 A-B). This is not surprising since sustained Erk activity was necessary for tubulogenesis in MDCK cells (54, 59). Although MEK signaling is important for tubulogenesis, results presented

here suggest that MEK signaling may not be essential for 4h activation of Rac1 or extension formation in organoids. These data indicate that Src and FAK mediate 4h Rac1 activity and extension formation in organoids.

Promogestone (R5020) reduces HGF-induced extensions and Rac1-GTP in mammary organoid tubulogenesis

To determine when R5020/PR signaling reduces tubulogenesis, the timing of the R5020 effect on tubulogenesis was analyzed (FIGURE 10 A-B). At 4h, R5020 significantly decreased the number of HGF-induced extensions. By 24h, HGF- and HGF+R5020-treated organoids had similar numbers of chains. However, the inclusion of R5020 significantly decreased the number of HGF-induced tubules. These results reveal that the R5020 effect on tubulogenesis in mammary organoids occurs by 4h.

The reduced extensions observed in HGF+R5020-treated organoids suggested Rac1-GTP might also be reduced. Indeed, HGF+R5020-treated organoids had lower Rac1-GTP than HGF-treated organoids (FIGURE 10 C). Because Src and FAK were necessary for Rac1-GTP and extension formation in tubulogenesis, the levels of phospho-Src and phospho-FAK were also analyzed. There was a trend for reduced phospho-Src and phospho-FAK in HGF+R5020-treated organoids. (FIGURE 10 D). However, the levels of phospho-Erk1/2 and phospho-AKT did not appear to be affected by R5020. These data suggest that R5020 decreases HGF-induced extensions through reduced activation of Src, FAK and Rac1

R5020-regulated Laminin-5 reduces HGF-induced Rac1-GTP and tubulogenesis

Next, we investigated how R5020 reduced Src, FAK and Rac1 activity after HGF treatment. An important contributor to tubulogenesis is the ECM which can influence a cell's response to hormones and GFs. It was reported that MDCK cells embedded in collagen I (Col I)

form tubules in response to HGF, but do not when embedded in laminin (Lm)-1 rich Matrigel (67, 68). In previously published microarray analysis of mouse mammary organoids treated with R5020, Lm γ 2 (subunit of Lm-5) mRNA was upregulated (65). Also MCF7 human breast cancer cells cultured on Lm-1 have reduced Rac1-GTP compared those cultured on Col I (69). This led to the hypothesis that laminin acts as an R5020-induced paracrine factor to reduce Rac1-GTP level and extension formation in organoids undergoing tubulogenesis.

First, to determine if laminin could block tubulogenesis of mammary organoids, organoids were cultured in Matrigel and treated with BM, HGF, R5020 or HGF+R5020 (FIGURE 11 A). Compared to organoids in Col I, organoids in Matrigel were unable to make tubules. This was observed even after 7 days of treatment with HGF (data not shown). Thus, a laminin-rich environment has an inhibitory effect on HGF-induced tubulogenesis. To determine if laminin could alter HGF-induced Rac1-GTP, primary mammary epithelial cells were cultured on Col I or Lm-1 coated plates and treated with HGF for 4h (FIGURE 11 B). HGF failed to increase Rac1-GTP in cells cultured on Lm-1 compared to cells on Col I. These results suggested that altered composition of the ECM can modulate the HGF-response.

Elevated Lm γ 2 protein level in response to R5020 treatment was then verified by immunoblot of organoid extracts and in-gel antibody labeling of intact organoids after 4h and 24h treatment (FIGURE 12 A-C). Lower levels of Lm γ 2 were observed for HGF-treated organoids. The combination of HGF and R5020 resulted in an intermediate level of Lm γ 2 (FIGURE 12 B-C). These results are consistent with our previous report that R5020 induced Lm γ 2 mRNA expression and indicates that R5020 signaling might alter the ECM composition.

To determine if R5020-increased Lm γ 2 is a paracrine factor responsible for stunted tubulogenesis, organoids were infected with adenovirus to deliver a GFP+ Lm γ 2-shRNA vector

or GFP+ Scramble control. Following knockdown, organoids were treated with HGF or HGF+R5020 and the effect on morphology and Rac1 activity was assessed (FIGURE 13 A-D). Compared to HGF+R5020 controls, organoids that had been infected with Lm γ 2-shRNA were able to produce significantly more tubules at 24h suggesting that extensions were also increased. However, an increase of extensions at 4h was not observed. It is likely that infection with adenovirus alters the tubulogenesis time-course of mammary organoids. The percentage of organoids with long tubules was higher in Lm γ 2-shRNA treated organoids compared to the HGF+R5020-treated controls. In addition, there was a trend for increased Rac1-GTP and phospho-Src in Lm γ 2-shRNA treated organoids compared to HGF+R5020 controls. Quantitative RT-PCR was performed to verify knockdown of Lm γ 2 mRNA, and showed a 3-fold reduction of Lm γ 2 mRNA compared to scramble controls (Table 1). Taken together, these results suggest that Lm-5 is an R5020-mediated paracrine factor that inhibits HGF-induced tubulogenesis through inhibition of Src and Rac1.

Lm-5 signals through α 6 β 1 and α 6 β 4 integrins. As further support that Lm-5 negatively regulates tubulogenesis in mammary organoids, α 6-integrin was blocked using a neutralizing antibody (FIGURE 14 A-D). The organoids were then treated with HGF or HGF+R5020 and the effect on tubulogenesis was analyzed. There was a trend for increased number of extensions, chains and tubules after blocking α 6 integrins in HGF+R5020 treated organoids. In addition, it appeared that a higher percentage of HGF+R5020-treated organoids were able to produce long tubules in the presence of the α 6-integrin blocking antibody compared to HGF+R5020 controls at 24h. This suggested that blocking α 6-integrin might also prevent the R5020-blunting effect of tubulogenesis. Furthermore, there was a trend for increased Rac1-GTP and phospho-Src after blocking α 6-integrin in HGF+R5020-treated organoids. These results are consistent with the

interpretation that R5020 upregulates Lm-5/ α 6-integrin signaling which appears to have an inhibitory effect on Src and Rac1 resulting in blunted extension formation and tubulogenesis.

CHAPTER 4

DISCUSSION

It is known that P is important for sidebranching and alveologenesis in development of the mammary gland. Yet, the mechanism of how P mediates sidebranching is not well understood. Using a 3D cell culture model of mammary gland ductal development and sidebranching, it was determined that HGF/c-Met activates Src, FAK and Rac1 pathway to promote extension formation, the first step in in vitro ductal elongation. It was found that activation of this pathway is reduced by R5020 to produce fewer extensions and stunted tubule formation, representing shortened ducts of sidebranches. In addition, it was determined that this is mediated by R5020-induced changes in laminin expression.

HGF activates a Src/FAK-Rac1 pathway to affect early tubule morphology

As a first step to identifying how R5020 blunts the tubulogenic response of organoids to HGF, the key pathway controlling early steps in tubule formation was determined. It was observed that HGF induced extension formation, the first step of tubulogenesis, occurred by 4h, and that Rac1-GTP was elevated at this time. Through the use of shRNA and an inhibitor against Rac1, the GTPase was identified as a regulator of extension and chain formation. For MDCK cells, extension formation and tubulogenesis were mediated through Rac1 signaling (57). It appears that mammary organoids, composed of two cell types, behave similarly to MDCKs in tubulogenesis. We have previously reported that LECs rather than MECs form extensions (11). Therefore it is likely that Rac1-induced changes during extension formation is occurring mainly in the LECs.

Using specific inhibitors, Src and FAK were identified as key regulators of Rac1 activity and extension formation in tubulogenesis. Although HGF-induced Src had been implicated in motility and proliferation of mouse mammary carcinoma cells (62), a role for Src in tubulogenesis of normal mouse mammary cells had not been established. Inhibition of Src reduced Rac1-GTP levels and severely impaired extension formation, suggesting that Src is upstream of Rac1 in tubulogenesis. Inhibition of FAK resulted in a similar reduction of extensions and Rac1-GTP. FAK and Src have been documented to cooperate at focal adhesions and to mediate both integrin and RTK signaling (70). Therefore, it is likely that both kinases interact upstream of Rac1 to mediate extension formation of organoids. Interestingly, a role for Src in tubulogenesis in MDCK cells has not been reported. In contrast, MEK and PI3K mediate cell migration and tubulogenesis of MDCK cells (54, 60, 61, 71). However, MEK and PI3K inhibition failed to significantly reduce Rac1-GTP levels and extension formation in the present study of mammary organoids. It is probable that these kinases contribute to later stages of tubulogenesis of mammary organoids but are nonessential for Rac1-induced extension formation.

R5020 reduces the Src-Rac1 pathway and extension formation

R5020 reduced the number of extensions, the early stage of tubulogenesis, and decreased the level of Rac1-GTP in organoids treated with HGF+R5020. Furthermore, R5020 reduced the level of phosphorylated Src and FAK. Therefore it is likely that R5020 blunts HGF-induced tubulogenesis through inhibiting activation of the Src/FAK-Rac1 pathway. This early effect of R5020 contributes to the ultimate blunted morphology reported previously (10). To the best of our knowledge, this is first evidence of progestin regulating Rac1 to control tubulogenesis of primary mammary organoids.

R5020 increases Lm-5 expression to decrease HGF-induced tubulogenesis

The role of ECM composition was investigated based on information that (1) MDCK cells in laminin-rich Matrigel do not form tubules in response to HGF (67, 68), (2) that R5020 signaling induces expression of laminin mRNA in organoids in collagen (65), and (3) that breast cancer cells have reduced Rac1-GTP when cultured on Lm-1 (69). In the present study, it was found that Matrigel inhibited HGF-induced tubulogenesis and that Lm-1 reduced Rac1-GTP level in organoids. In addition, it was observed that R5020 increased expression of Lm γ 2 (subunit of Lm-5) in mammary organoids. When Lm γ 2 was silenced, Rac1-GTP, tubule length and number were restored, indicating that Lm-5 is an R5020-induced paracrine factor that negatively regulates tubulogenesis. Blocking α 6-integrin also restored Rac1-GTP and tubulogenesis in HGF+R5020-treated organoids, further confirming the role of Lm-5 signaling. Taken together, the present findings suggest that Lm-5/ α 6-integrin signaling is a negative regulator of tubulogenesis and Rac1-GTP, and that Lm-5/ α 6-integrin signaling contributes to shorter tubules observed in HGF+R5020 treated organoids. Since the adult mammary gland that was the source of our organoids express only PRA (11) we postulate that the effects of R5020 are mediated through PRA. These findings lead us to propose the following model of mammary organoid tubulogenesis and sidebranching (FIGURE 14). Under HGF treatment and increased Rac1-GTP, LECs in collagen I become motile and begin migration outwards to form tubules. However, in the presence of R5020, PRA upregulates Lm-5 and blunts the tubulogenic response to HGF through an Lm-5/ α 6-integrin and Rac1 mediated pathway. We interpret blunting of tubulogenesis to be a surrogate for the side branching response induced by P in vivo.

Non-genomic signaling of progestin in tubulogenesis

The effects of R5020 mediated by PRA are likely occurring through genomic signaling since RU486 blocks the R5020 inhibitory effect on tubulogenesis (10). However, it is important to note that other mechanisms might be at play in organoid sidebranching. One possibility is that R5020 might initiate a non-genomic PRA pathway in addition to a classical genomic pathway. There is evidence from human breast cancer cell lines that non-genomic signaling of PR influences activity of Src. PRB has been shown to interact with the SH3 domain of Src leading to activated MAPK signaling and higher proliferation of T47D cells (45, 72). In contrast to what was observed in breast cancer cells, R5020/PRA reduced the level of phosphorylated Src in mammary organoids. This difference might be a reflection of the lack of significant PRB in the adult virgin mouse mammary gland compared to the co-expression of PRA and PRB in human normal and cancerous breast cells. Additional differences might be due to culture of mammary organoids in collagen vs. human cancer cell lines on plastic.

Conclusion

In summary, we identified an ECM/integrin and HGF/cMet activated Src/FAK-Rac1 pathway that mediates extension formation as an early step of tubulogenesis in mammary organoids in vitro. This pathway was inhibited by R5020 and resulted in blunted tubulogenesis believed to be analogous to the sidebranching response to P in vivo. A potential mechanism was highlighted through which R5020 acting through PRA increases expression of extracellular laminin to blunt tubulogenesis. PRA has been considered by some to be non-essential in mammary gland development. However, in vivo studies of its expression during development (14, 49) and the findings presented here suggest that it may play an important role in sidebranching.

APPENDICES

APPENDIX A

PROGESTERONE RECEPTOR ISOFORM KNOCKOUTS

Introduction

The question of PRA function in mammary gland development has not been fully resolved. Isoform specific PR knockout mice revealed that PRB contributes to alveologenesis while PRA is important for normal uterine and ovary function (8, 47). However, the isoform knockouts were generated in the mixed genetic background of C57BL/6 x 129SV. C57BL/6 strain is known to have a delayed mammary gland development and reduced progesterone response compared to the Balb/c strain that is often used in studies of the gland (48, 73). Developmental studies from Balb/c suggest there might be a role for PRA in sidebranch development (11, 14, 49). Therefore, a role for PRA in mammary gland development may have been missed in the PRA knockout in C57BL/6 context. To address this, Balb/c DNA constructs for PRA-specific and PRB-specific knockouts were designed. C-Terminal epitope tags were included in the design to facilitate easy detection of PRA or PRB in developmental studies.

Materials and Methods

PRA- and PRB-knockout design

Targeting vectors were generated to create PR isoform specific mini genes with epitope tags. Vectors contained 5.5 Kb genomic Balb/C DNA with the PR promoters and exons 1-2. Site directed mutagenesis was used to mutate the separate PR initiation sites from ATG (Met) to GCG (Ala) for the PRAKO or CTG (Leu) for the PRBKO. A loxP-flanked PGK-Neo selection cassette (gift from Dr. Pam Swiatek) was inserted within intron 1. An HA tag or Flag tag was included at the C-terminal end of PR cDNA encoding exons 3-8. The HA-tagged cDNA was then added to exon 2 of the PRAKO vector while the Flag-tagged cDNA was added to exon 2 of the PRBKO vector. An SV40 polyadenylation sequence was included after the tagged cDNA and a 3' homologous recombination arm was added that consisted of 5 Kb of intron 2.

Recombination of the constructs with wild type PR DNA would replace the PR promoters and exons 1-2 with an isoform specific tagged mini PR gene, interrupting the wild type gene (FIGURE 15).

The PRAKO and PRBKO constructs were submitted to the University of Michigan Transgenic Animal Model Core (TAMC) for electroporation into Oz-Balb/C embryonic stem (ES) cells. G418 resistant clones were isolated by the TAMC. ES cell DNA received from the TAMC was analyzed by Southern blotting and PCR to identify PRAKO and PRBKO recombinants.

Southern blot and PCR analysis of recombinant ES cells

Two Bcl I restriction sites flank the endogenous PR gene resulting in a 15 Kb fragment when the DNA is digested with the restriction enzyme. Recombination with the PR mini genes introduces a two additional Bcl I restriction site within the Neo cassette and the cDNA portion of the constructs, resulting in 7.4 Kb, 3.6 Kb and 7.8 Kb fragments. A 510 bp 5' DNA probe was generated upstream of the 5' recombination site, and a 448 bp 3' DNA probe was created downstream of the 3' recombination site. The 5' and 3' probes recognize the 7.4 Kb and 7.8 Kb fragments, respectively.

ES DNA on 96-well plates was digested overnight with Bcl I (20 U; Roche Diagnostics, Indianapolis, IN) and RNase I (50 µg/mL) in a humidified chamber. DNA was separated by electrophoresis overnight on a 0.8% agarose gel. DNA within the gel was depurinated in 0.25 N HCl for 15 minutes, rinsed in ddH₂O, and denatured in 0.5 N NaOH for 30 minutes. DNA was transferred in 10x SSC (1.5 M sodium chloride, 1.5 M sodium citrate, pH 7.0) by vacuum blotting to Hybond-N nylon membrane (GE-Amersham, Piscataway, New Jersey) using 785 Vacuum Blotter (BioRad, Hercules, CA) at 5 inches Hg. The membrane was washed with 2x

SSC and baked 1 hour at 65°C and wetted with 2x SSC and pre-hybridized with QuikHyb hybridization solution (Stratagene, La Jolla, CA) 30 minutes at 65°C prior to hybridization.

DNA probes were labeled with (α -³²P)dCTP using Random Primer Labeling Kit as per manufacturers recommendation (Invitrogen, Carlsbad, CA). Labeled probes were purified using Chroma Spin columns (Clontech, Mountain View, CA). Probes were boiled with 10 mg/mL sonicated herring sperm DNA, and added to QuikHyb hybridization solution. Probes were hybridized to the membrane overnight at 55°C. The membrane was washed the following day twice for 15 minutes at room temperature with 2x SSC and 0.1% SDS and washed once for 30 minutes at 55°C with 2x SSC and 0.1% SDS. Membranes were exposed to a PhosphorImaging screen (GE Healthcare Biosciences), and scanned using a Storm Molecular Imager (GE Healthcare Biosciences). Because of difficulties in analyzing the 3' recombination event in PRAKO clones by Southern blots, PCR analysis was used to confirm the presence of the HA epitope tag.

Generation of chimeric mice

Recombinant ES cells were expanded by the TAMC and chromosomes were counted to verify euploid chromosome numbers. Clones were injected into C57BL/6NCrl x (C57BL/6J X DBA/2J) blastocysts by the TAMC resulting in PRAKO- and PRBKO- chimeric mice. Chimeric mice were put into breeding with Balb/c mice to generate Balb/c PRAKO +/- and PRBKO +/- mice.

PCR Genotyping

For screening the 5' end of the PRAKO and PRBKO allele, primers were generated flanking the start sites. PCR generates a 1289 bp product for both wild type (WT) and mutant alleles. Following PCR amplification, the products are digested with Bsp HI to distinguish WT allele from mutant alleles. For screening the 3' end of the PRAKO and PRBKO allele, primers were designed to amplify a region of intron 2. The primers flank the insertion site of the SV40 polyadenylation signal. The size of the PCR product was used to distinguish the WT allele from mutant alleles.

Results

PRA and PRB are encoded within a single gene containing two promoter sites. In order to create PRA knockout and PRB knockout Balb/c mice, targeting vectors were generated that introduce a PRA-specific or PRB-specific mini-gene into the WT PR locus (FIGURE 15). The 5' recombination arm consisted of the Balb/c PR promoter through exon 1. The ATG sites for PRA or PRB were mutated so that only one isoform would be expressed. A loxP-flanked Neomycin (Neo) selection cassette was included within intron 1 for selection of recombinant ES cells. Epitope tagged cDNA encoding exons 3-8 was fused to exon 2 to complete the PR mini-genes. Presence of an HA- or Flag-epitope tag will make it easy to identify PRA or PRB protein in future PRAKO or PRBKO mice. Finally, the 3' recombination arm consisted of DNA from within intron 2 and included an SV40 polyadenylation signal. These targeting vectors should replace the WT promoter and exons 1-2 and interrupt the WT PR gene after homologous recombination. The endogenous PR exons 3-8 remain.

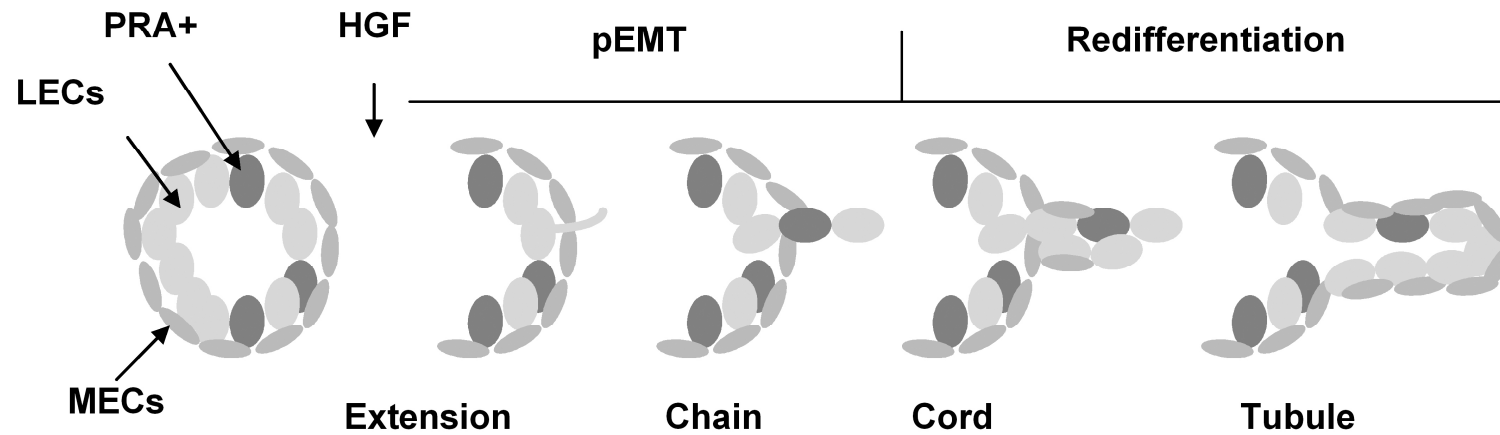
After the targeting vectors were introduced into OZ-Balb/c ES cells, Neo-containing ES cells were screened by Southern blotting and PCR analysis to identify correct recombinants. 2

PRA knockout ES clones and 3 PRB knockout clones were identified by Southern blot analysis (FIGURE 16). These were validated by PCR analysis using primers specific for the epitope tags. These clones were injected into C57BL/6NCrl x (C57BL/6J X DBA/2J) blastocysts resulting in 14 PRBKO chimeric mice and 11 PRAKO chimeric mice. The chimeras were put into breeding with wt Balb/c and germline PRB^{-/+} Balb/c have been identified by PCR genotyping (FIGURE 17). These animals have been put into breeding to amplify the colony. Heterozygote-heterozygote breeding will be done to generate homozygous PRB^{-/-} mice. To date, no PRA^{-/+} heterozygotes have been identified from breeding of the chimeric PRA^{-/+} animals.

APPENDIX B

FIGURES

FIGURE 1

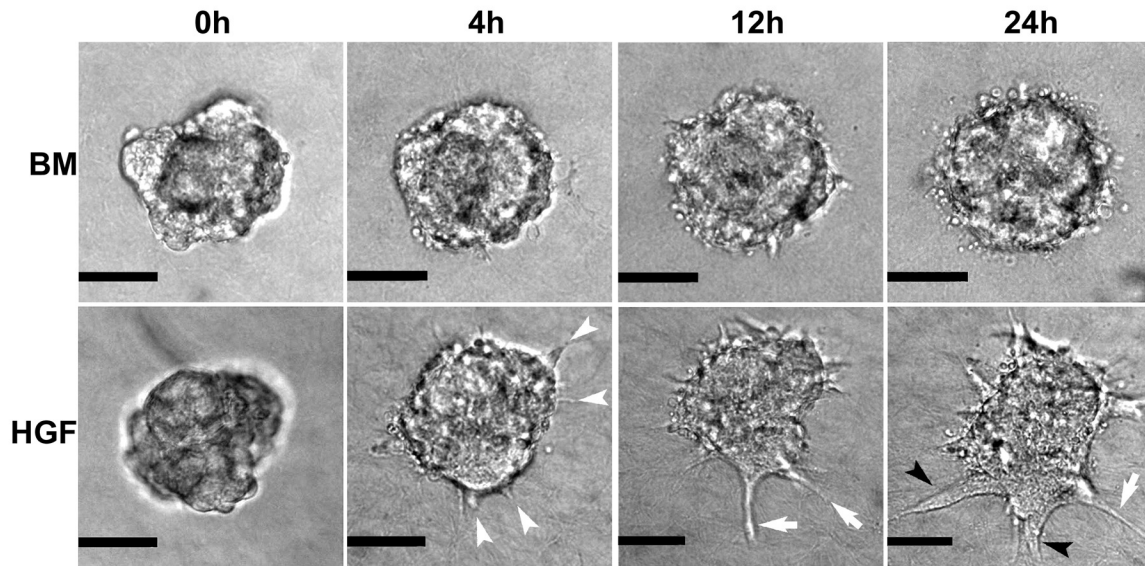


Tubulogenesis of mammary organoids.

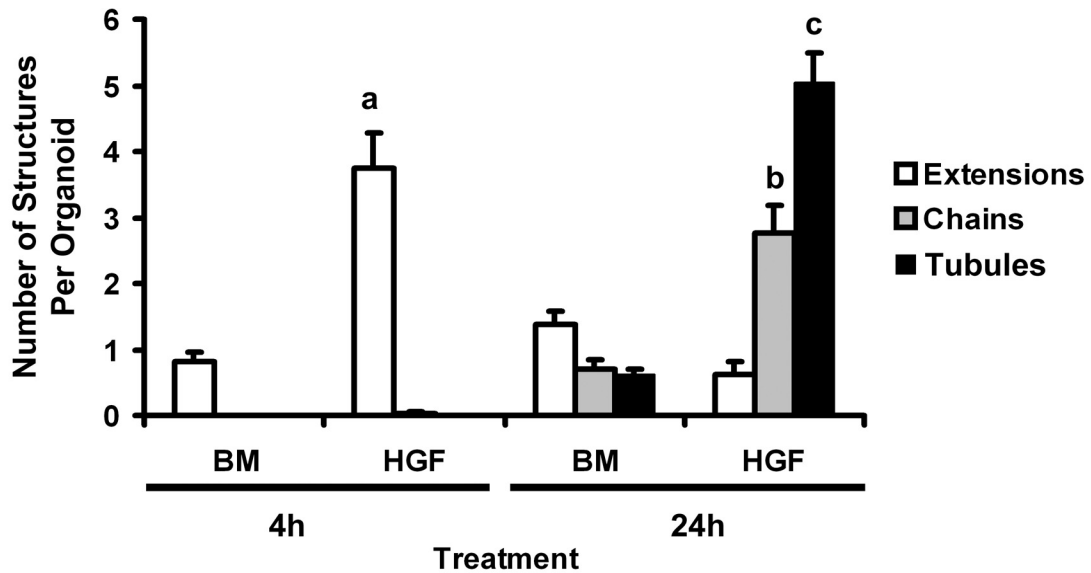
Organoids are composed of progesterone receptor-A positive (PRA+) and negative luminal epithelial cells (LECs) surrounded by myoepithelial cells (MECs). In the presence of hepatocyte growth factor (HGF), LECs undergo a partial epithelial-to-mesenchyme transition (pEMT) and form cytoplasmic extensions and single layer chains of cells to invade the surrounding matrix. Cells redifferentiate to form bi-layered cords with a discontinuous lumen, and finally a mature tubule with a complete lumen.

FIGURE 2

A



B

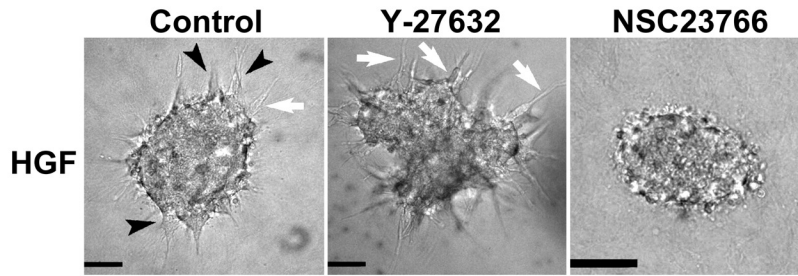


Time course of morphological changes induced by HGF.

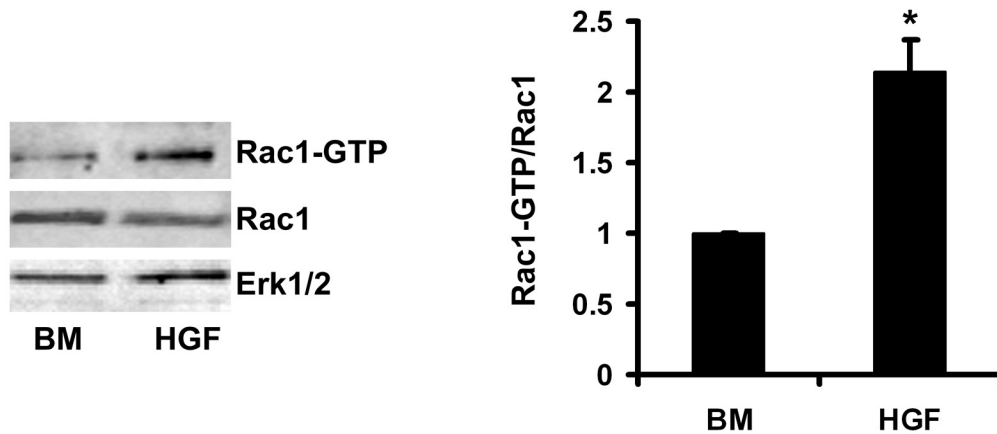
Organoids were treated with BM control or HGF (50 ng/ml) for up to 24h. A). Representative phase contrast micrographs of organoids at 0,4,12 and 24h. White arrowheads indicate extensions, white arrows indicate chains and black arrowheads indicate tubules. Scale bar = 0.05mm. B). Quantitation of extensions, chains and tubules at 4 or 24h treatment. a, b, c, $p < 0.05$ that HGF treatment increased indicated structures compared to BM (n = 10).

FIGURE 3

A



B

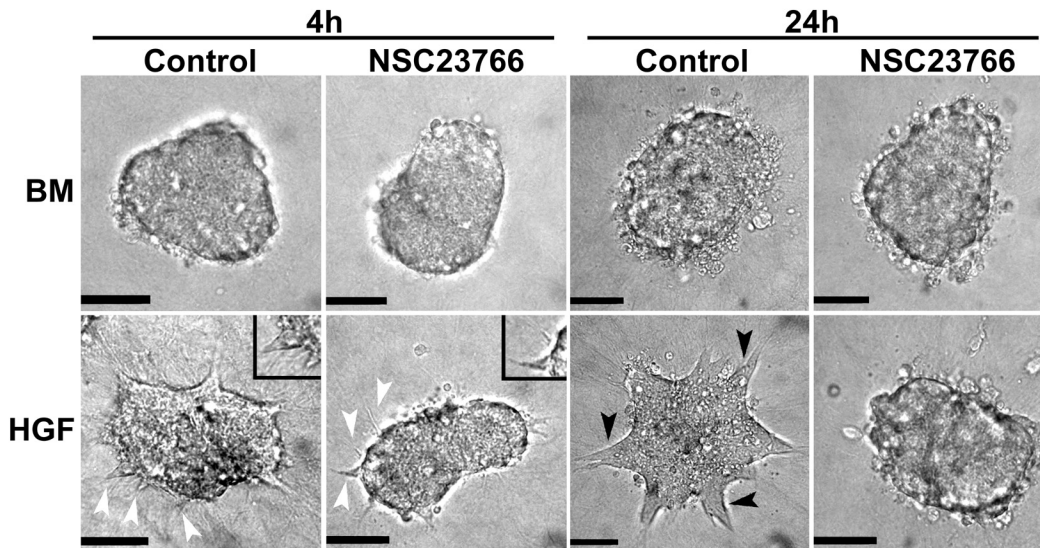


The effect of Rho or Rac1 inhibition on HGF-induced tubulogenesis.

Organoids were treated with HGF (50 ng/ml) in the presence or absence of the Rho kinase inhibitor (Y-27632; 50 μ M) or the Rac1 inhibitor (NSC23766; 100 μ M) for 24h. A). Representative phase contrast micrographs of organoids at 24h. White arrows indicate chains and black arrowheads indicate tubules. Scale bar = 0.05mm. B). Activation of Rac1 by HGF. Rac1-GTP levels were analyzed at 4h by Rac1-GTP pull down and immunoblot. For densitometry, Rac1 was normalized to total Rac1 and fold change relative to BM was calculated. *, $p < 0.05$ HGF Rac1-GTP greater than BM Rac1-GTP (n = 7).

FIGURE 4

A



B

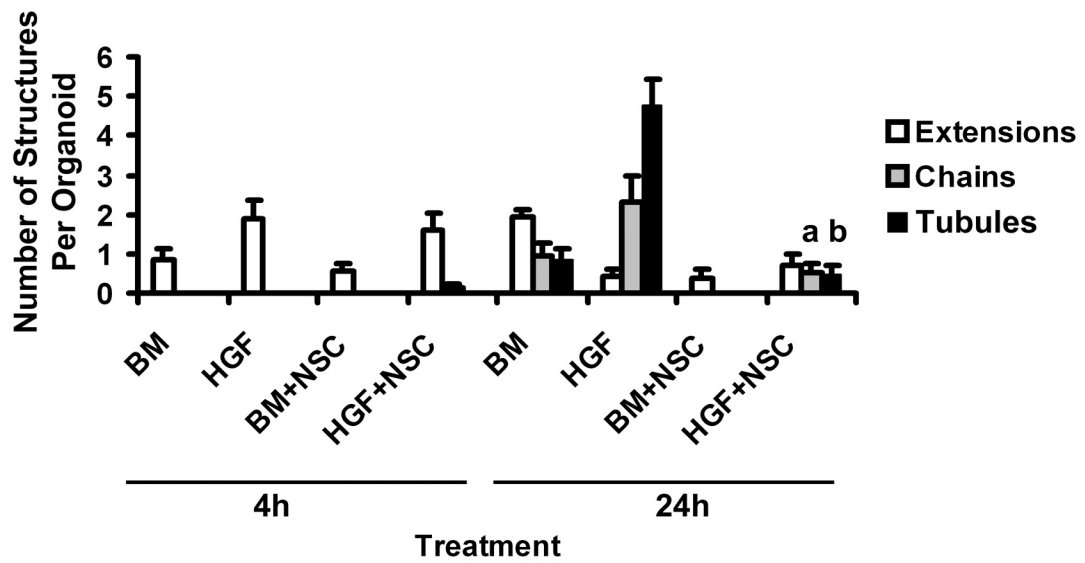
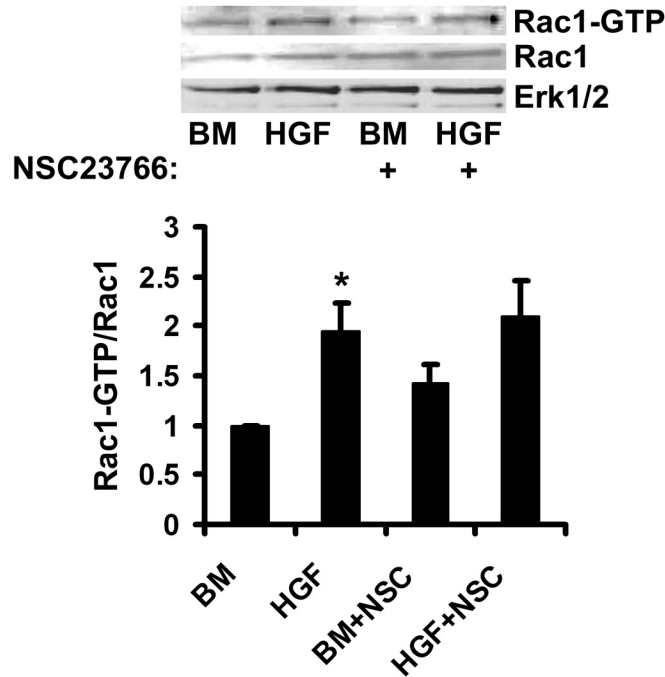


FIGURE 4 (cont'd)

C

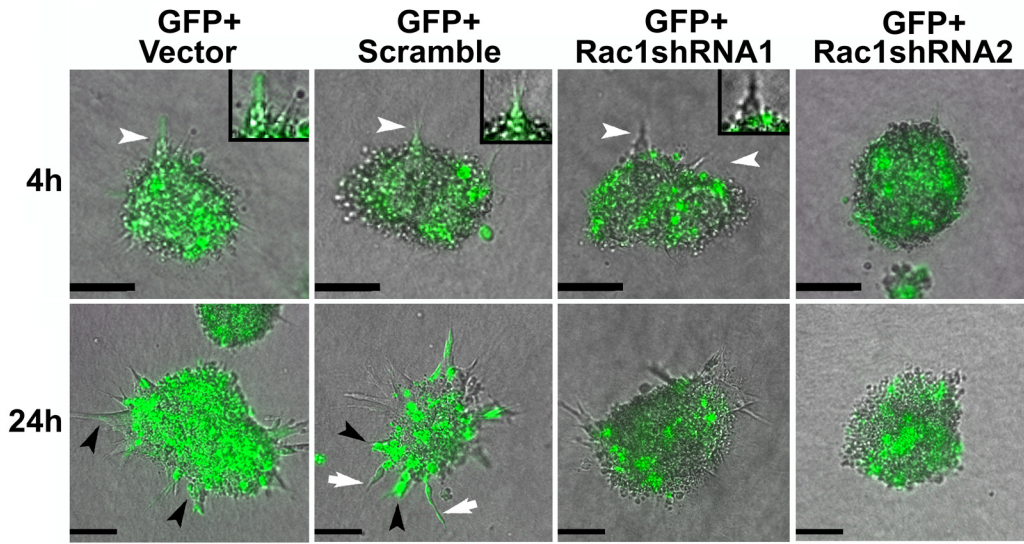


Rac1 inhibition reduces HGF-induced tubulogenesis.

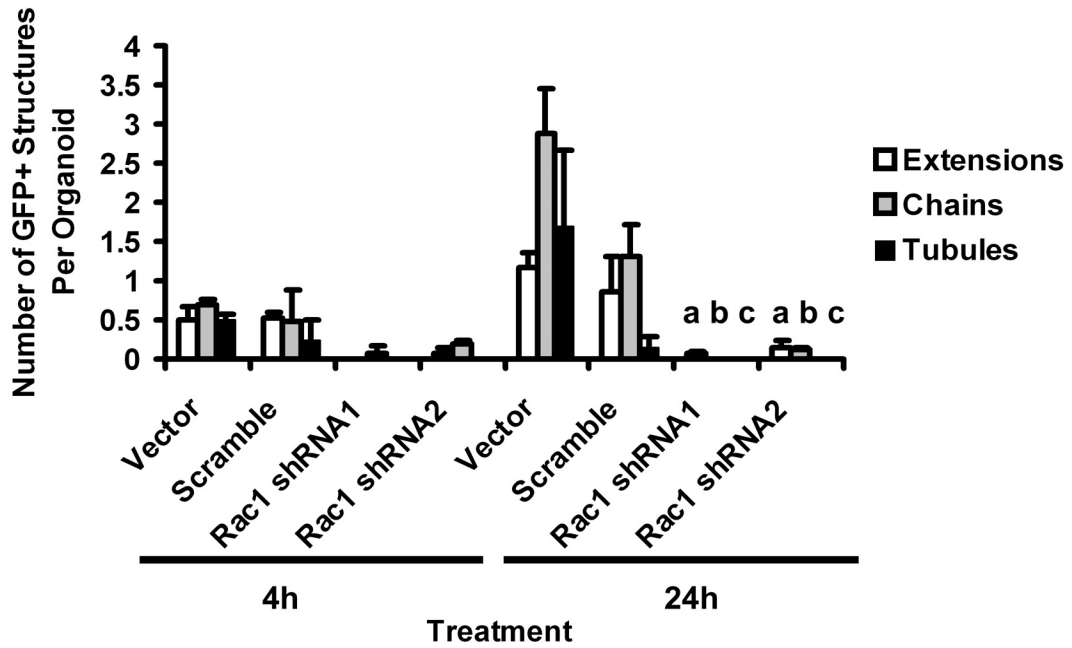
Organoids were treated with BM or HGF in the presence or absence of Rac1 inhibitor (NSC23766; 100 μ M) for 24h. A). Representative phase contrast micrographs of organoids at 4 and 24h. White arrowheads indicate extensions, and black arrowheads indicate tubules. Scale bar = 0.05mm. B). Quantitation of extensions, chains and tubules after 4 and 24h treatment with the Rac1 inhibitor. a,b, $p < 0.05$ that indicated structures are reduced by inhibitor (n = 4). C). Analysis of active Rac1 at 4h after treatment with inhibitor. Rac1-GTP levels were analyzed by Rac1-GTP pull down and immunoblot. For densitometry, Rac1-GTP was normalized to total Rac1 and fold change relative to BM was calculated. *, $p < 0.05$ HGF Rac1-GTP greater than BM Rac1-GTP (n = 4).

FIGURE 5

A



B



C

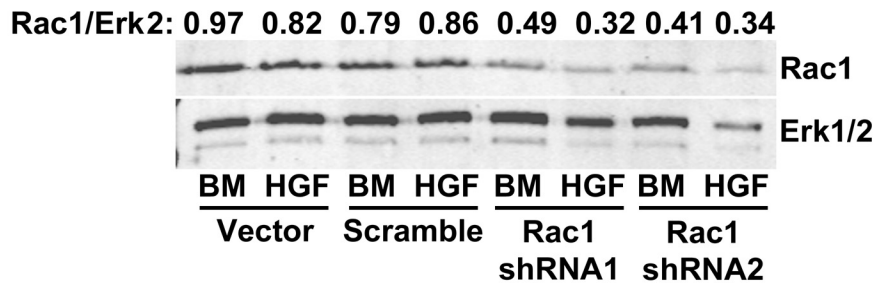


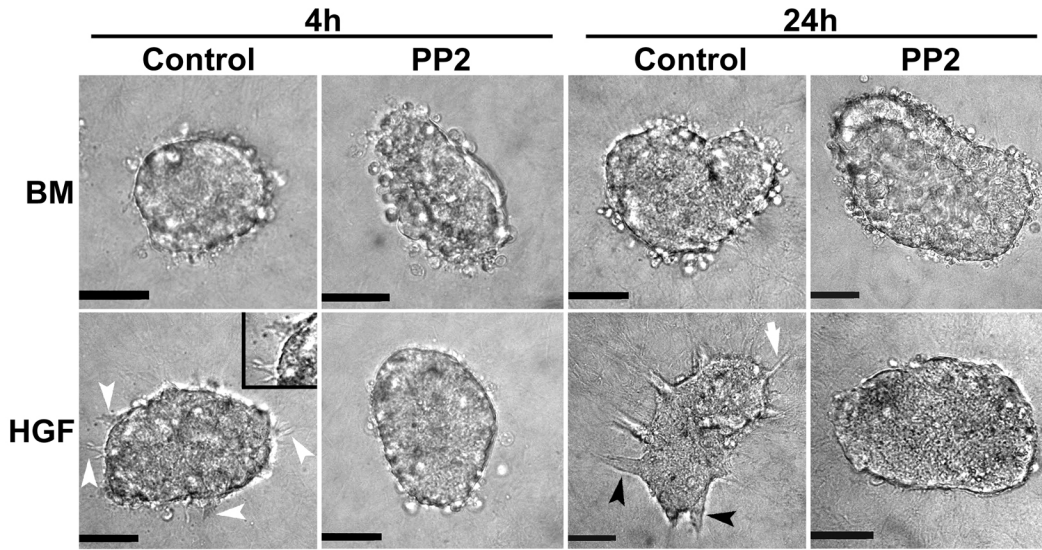
FIGURE 5 (cont'd)

Rac1 shRNA blocks HGF-induced tubulogenesis

For interpretation of the references to color in this and all other figures, the reader is referred to the electronic version of this dissertation. Organoids were infected with control virus (GFP+ Vector and GFP+ Scramble) or virus carrying shRNA against Rac1 (GFP+ Rac1shRNA1 and GFP+ Rac1shRNA2). At 48h post infection, organoids were treated with HGF for 24h. A). Representative phase contrast and GFP overlay images of organoids at 4 and 24h. White arrowheads indicate extensions, white arrows indicate chains and black arrowheads indicate tubules. Insets are enlargements of GFP+ and GFP-extensions. B). Quantitation of extensions, chains and tubules at 4 or 24h. a,b,c $p < 0.05$ that the numbers of indicated structures are reduced by Rac1shRNA compared to vector control. 30-50 organoids were analyzed per treatment from two separate experiments. C). Immunoblot of total Rac1 at 4h after treatment with BM or HGF. For densitometry, Rac1 was normalized to total Erk1/2.

FIGURE 6

A



B

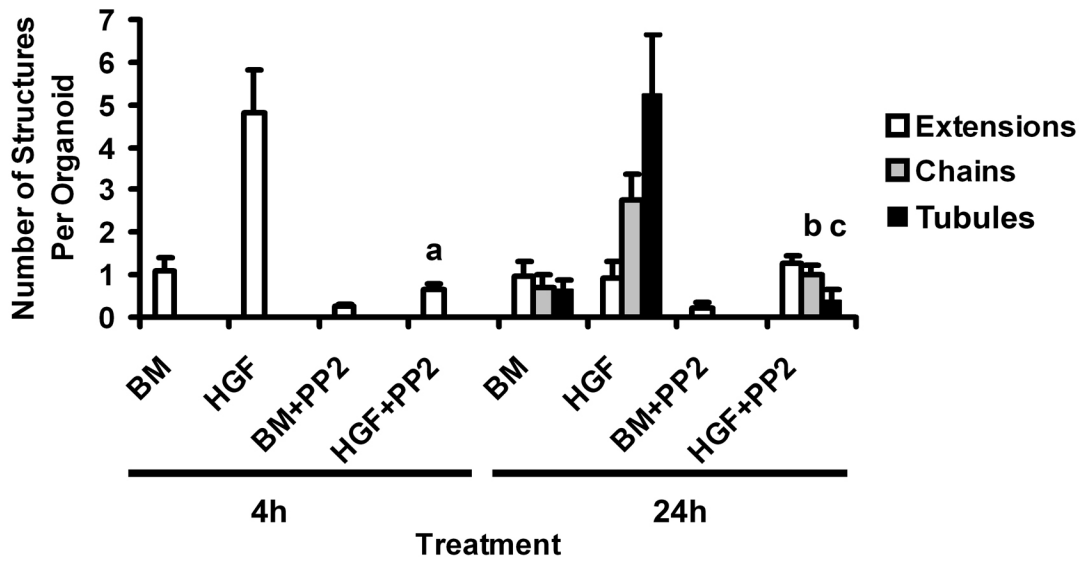
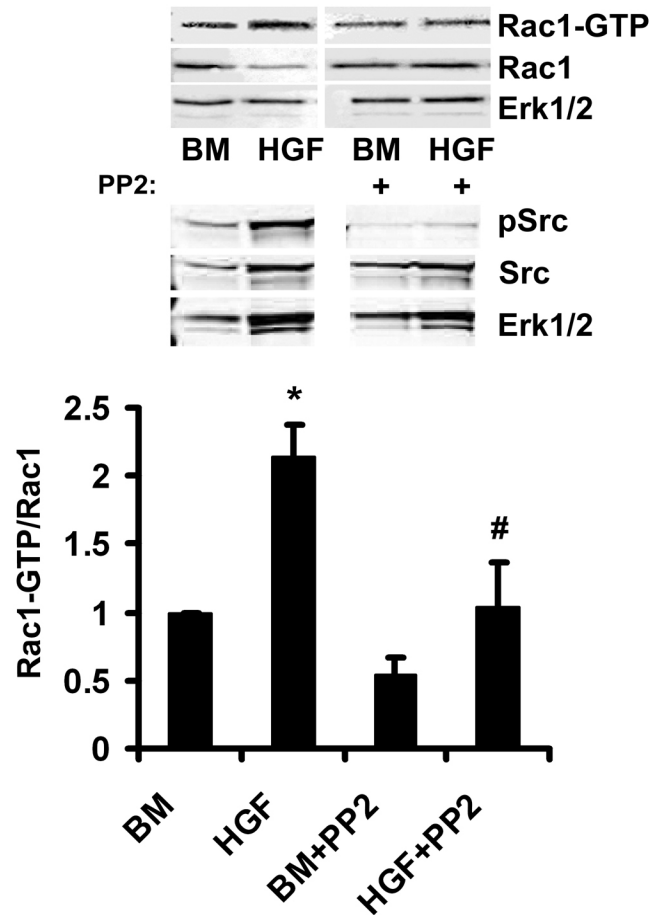


FIGURE 6 (cont'd)

C

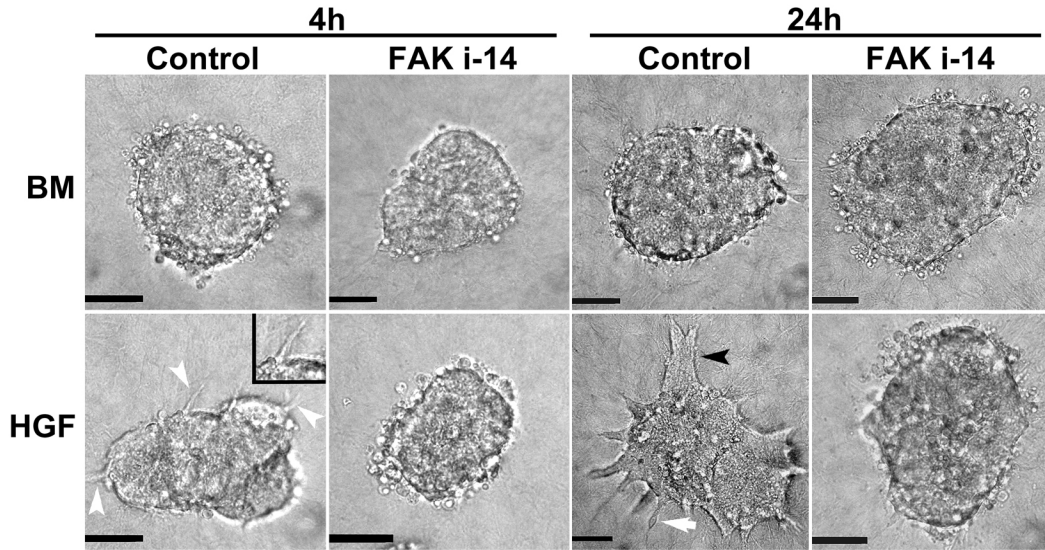


Src inhibition blocks HGF-induced tubulogenesis.

Organoids were treated with BM or HGF in the presence or absence of the Src inhibitor (PP2; 20 μ M) for 24h. A). Representative phase contrast micrographs of organoids at 4 and 24h. White arrowheads indicate extensions, white arrow indicates a chain and black arrowheads indicate tubules. Scale bar = 0.05mm. B). Quantitation of extensions, chains and tubules after 4 and 24h treatment with the PP2 inhibitor. a,b,c $p < 0.05$ that PP2 inhibitor decreased the numbers of indicated structures compared to controls ($n = 3$). C). Rac1-GTP levels were analyzed by Rac1-GTP pull down and immunoblot; phospho-Src levels were analyzed by immunoblot. For densitometry, Rac1-GTP was normalized to total Rac1 and fold change relative to BM was calculated. * $p < 0.05$ HGF Rac1-GTP greater than BM Rac1-GTP. # $p < 0.05$ Src inhibitor reduced HGF Rac1-GTP ($n = 3$).

FIGURE 7

A



B

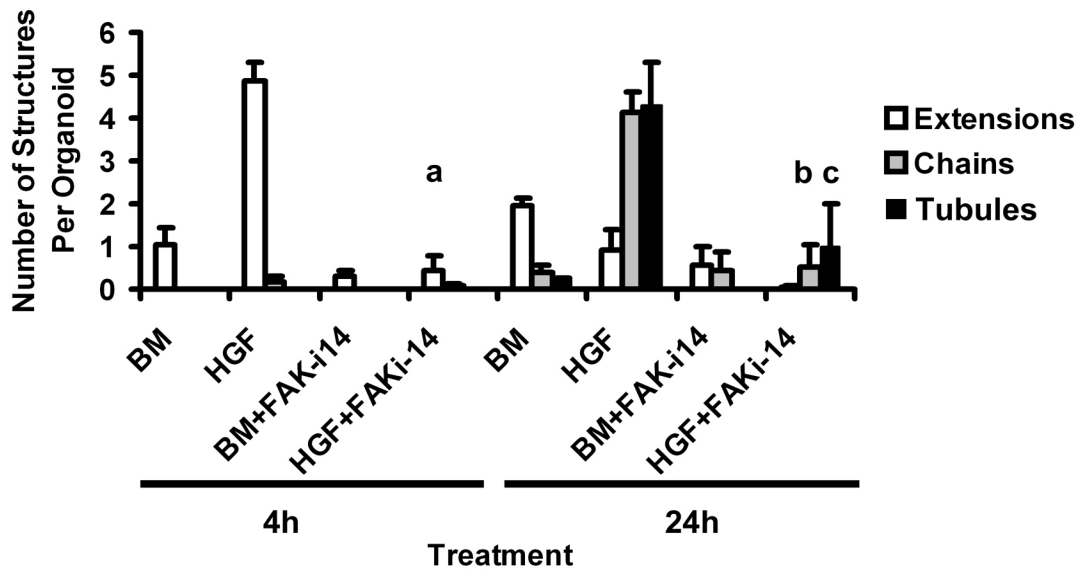
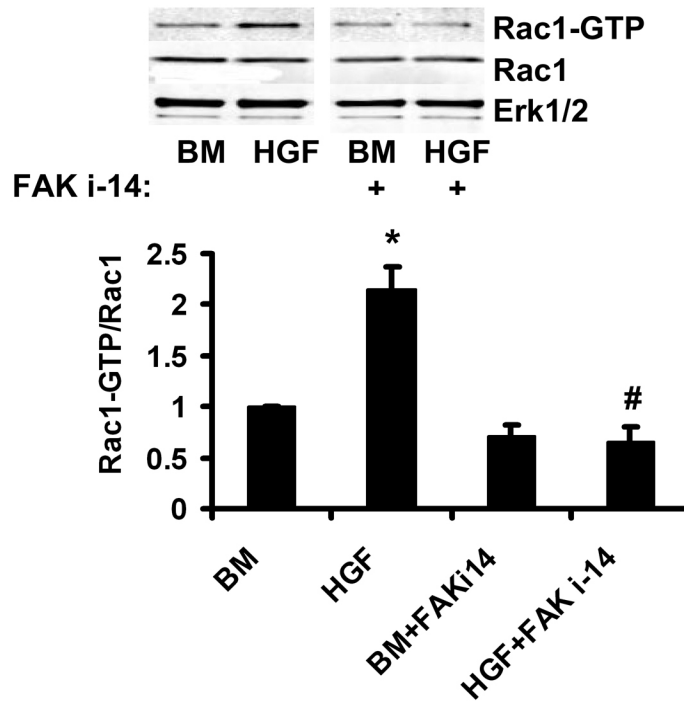


FIGURE 7 (cont'd)

C

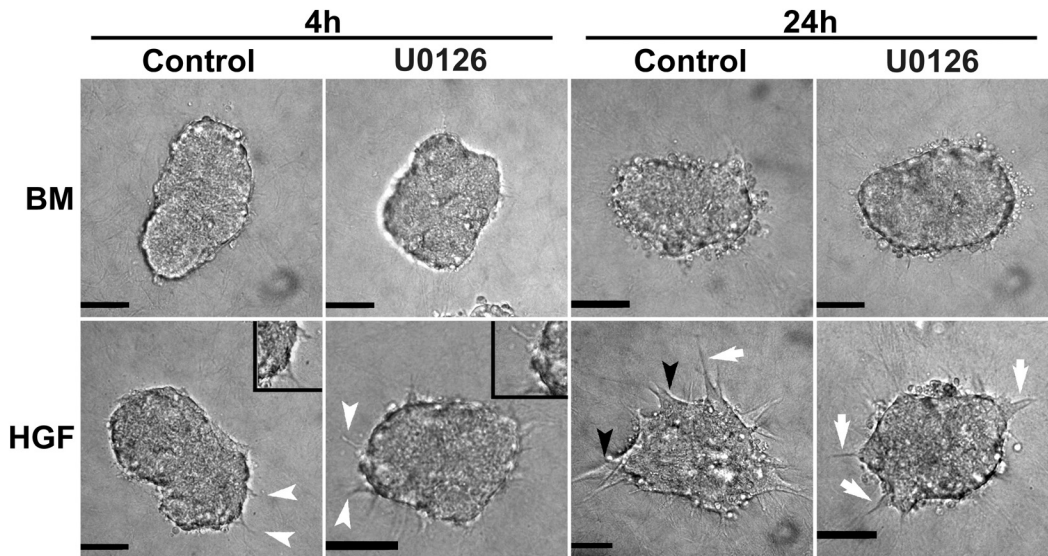


FAK inhibition blocks HGF-induced tubulogenesis.

Organoids were treated with BM or HGF in the presence or absence of the FAK inhibitor (FAK i-14; 10 μ M) for 24h. A). Representative phase contrast micrographs of organoids at 4 and 24h. White arrowheads indicate extensions, white arrow indicates a chain and black arrowhead indicates a tubule. Scale bar = 0.05mm. B). Quantitation of extensions, chains and tubules after 4 and 24h treatment with the FAK inhibitor. a,b,c, $p < 0.05$ that FAK inhibitor reduced the numbers of indicated structures compared to controls ($n = 3$). C). Rac1-GTP levels were analyzed after 4h by Rac1-GTP pull down and immunoblot. For densitometry, Rac1-GTP was normalized to total Rac1 and fold change relative to BM was calculated. * $p < 0.05$ HGF Rac1-GTP greater than BM Rac1-GTP. # $p < 0.05$ FAK inhibitor reduced HGF Rac1-GTP ($n = 3$).

FIGURE 8

A



B

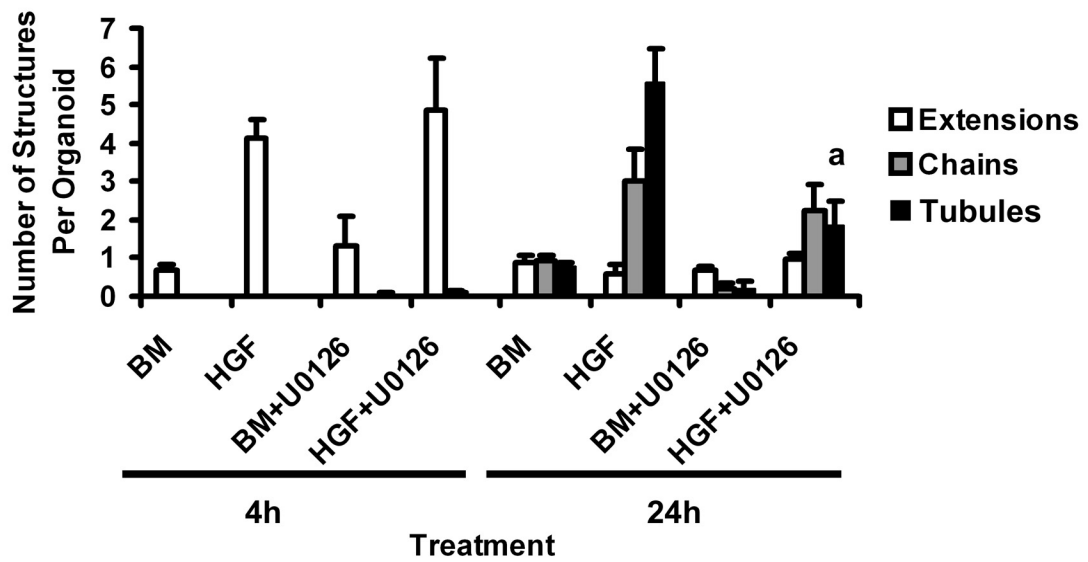
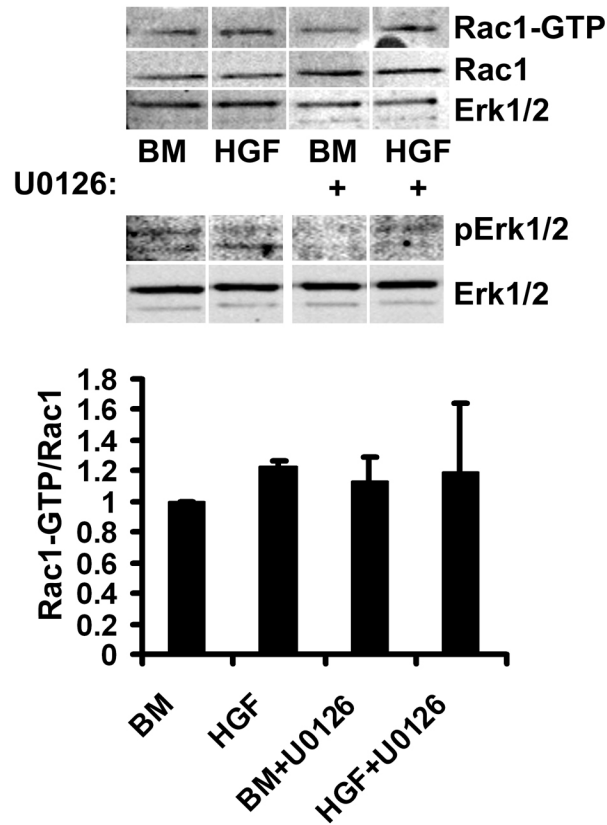


FIGURE 8 (cont'd)

C

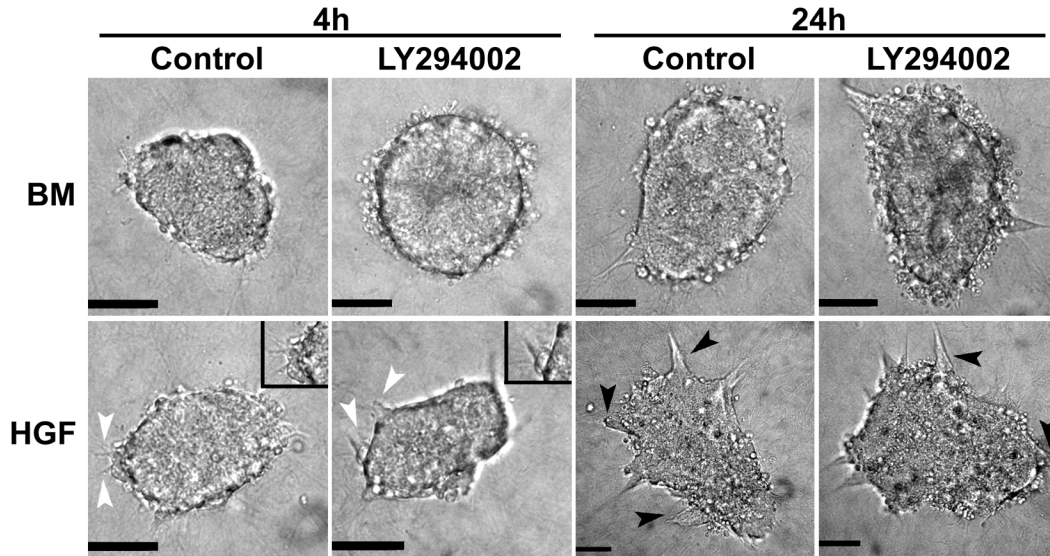


The effect of MEK inhibition on HGF induced tubulogenesis.

Organoids were treated with BM or HGF in the presence or absence of the MEK inhibitor (U0126; 10 μ M) for 24h. A). Representative phase contrast micrographs of organoids at 4 and 24h. White arrowheads indicate extensions, white arrows indicate chains and black arrowheads indicate tubules. Scale bar = 0.05mm. B). Quantitation of tubules after 4 and 24h treatment with the MEK inhibitor. a, $p < 0.05$ that MEK inhibitor reduced chains compared to controls ($n = 4$). C). Effect of MEK inhibition on Rac1 activity. Rac1-GTP levels were analyzed at 4h by Rac1-GTP pull down and immunoblot; phospho-Erk was analyzed by immunoblot. For densitometry, Rac1-GTP was normalized to total Rac1 and fold change relative to BM was calculated ($n = 2$).

FIGURE 9

A



B

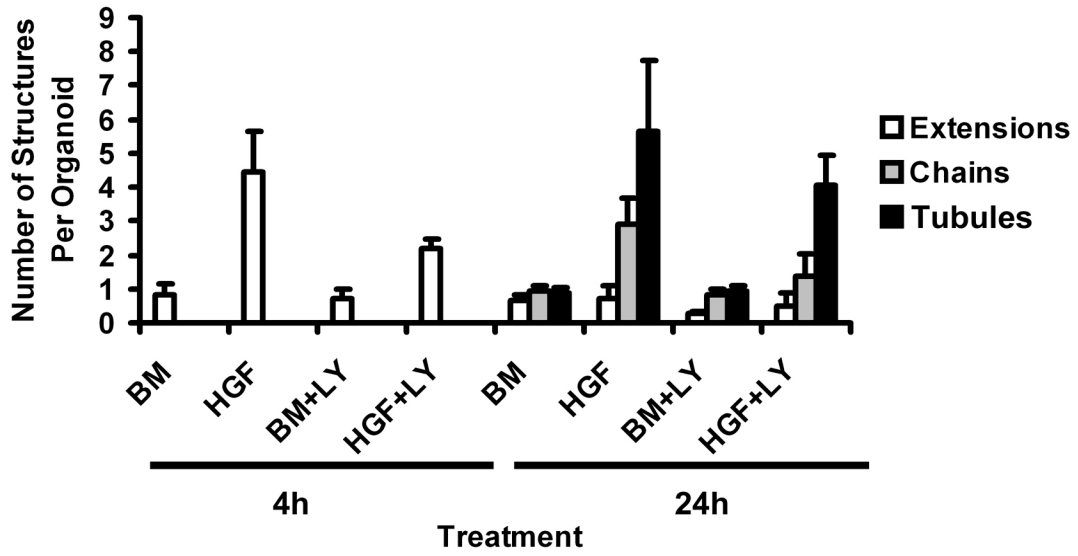
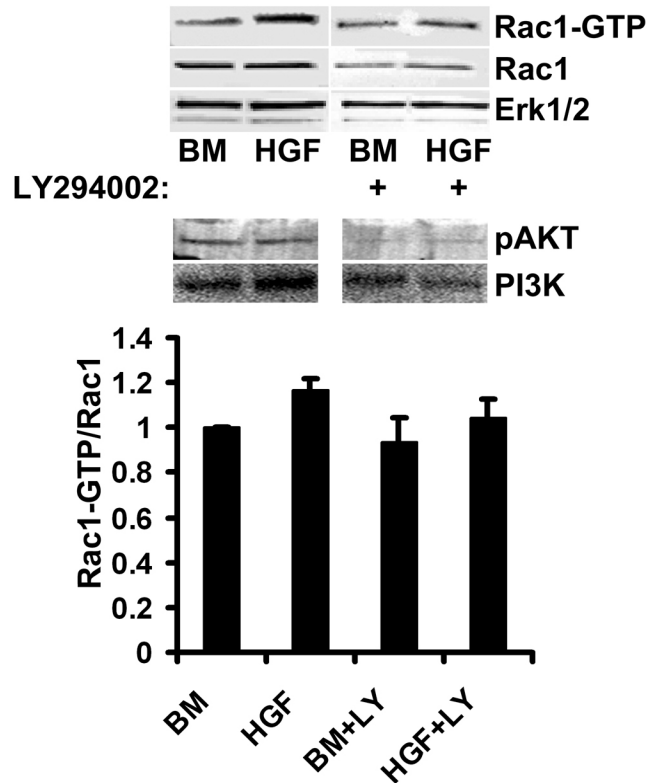


FIGURE 9 (cont'd)

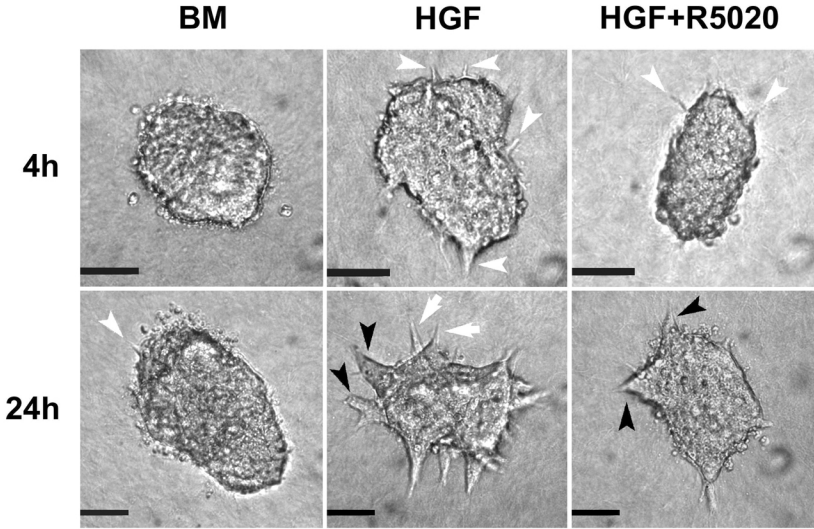
C



The effect of PI3K inhibition on HGF-induced tubulogenesis. Organoids were treated with BM or HGF in the presence or absence of the PI3K inhibitor (LY294002; 10 μ M) for 24h. A). Representative phase contrast micrographs of organoids at 4 and 24h. White arrowheads indicate extension and black arrowheads indicate tubules. Scale bar = 0.05mm. n = 3 B). Quantitation of extensions, chains and tubules after 4 and 24h treatment with the PI3K inhibitor (n = 3). C). Rac1-GTP levels were analyzed at 4h by Rac1-GTP pull down and immunoblot; phospho-AKT was analyzed by immunoblot. For densitometry, Rac1-GTP was normalized to total Rac1 and fold change relative to BM was calculated (n = 4).

FIGURE 10

A



B

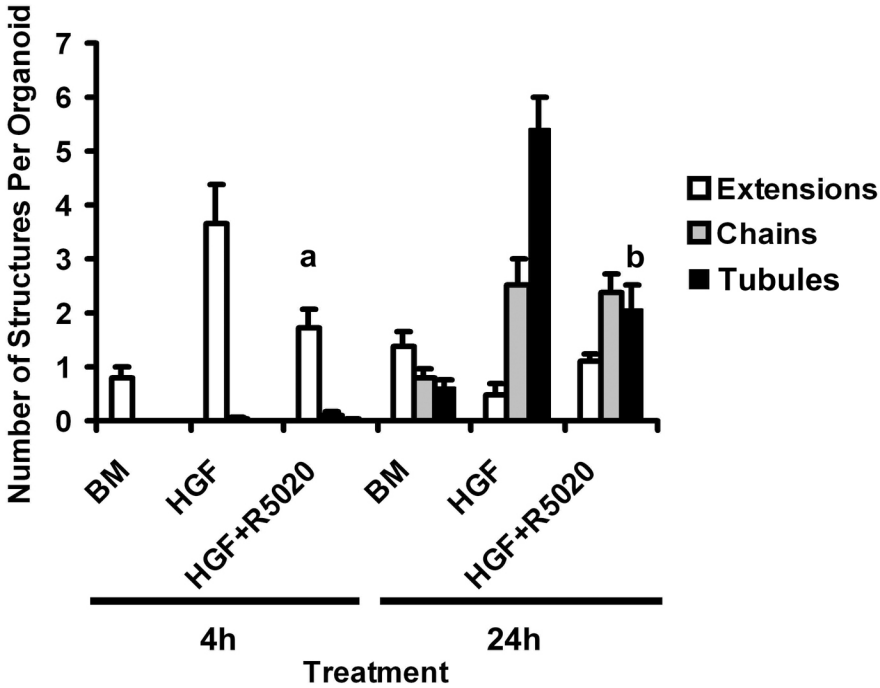
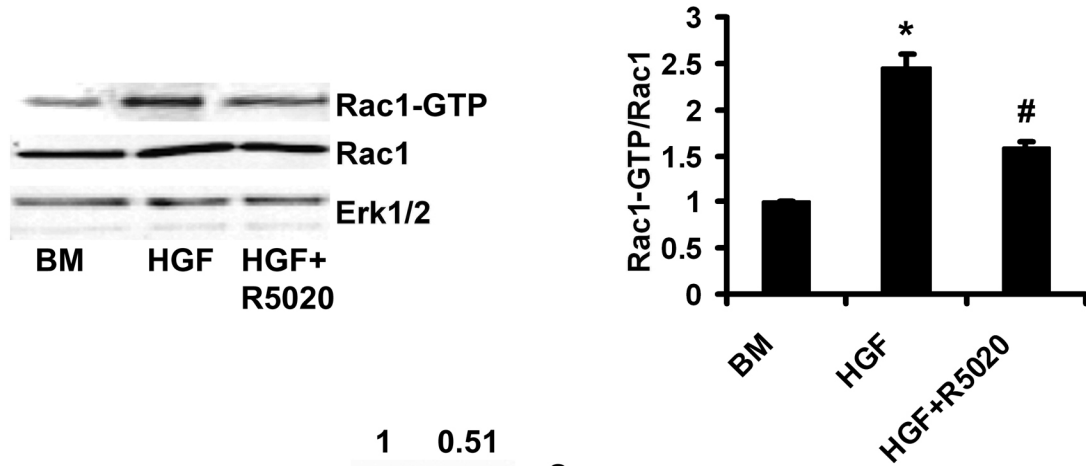
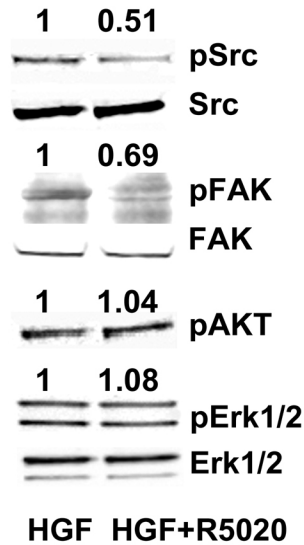


FIGURE 10 (cont'd)

C



D

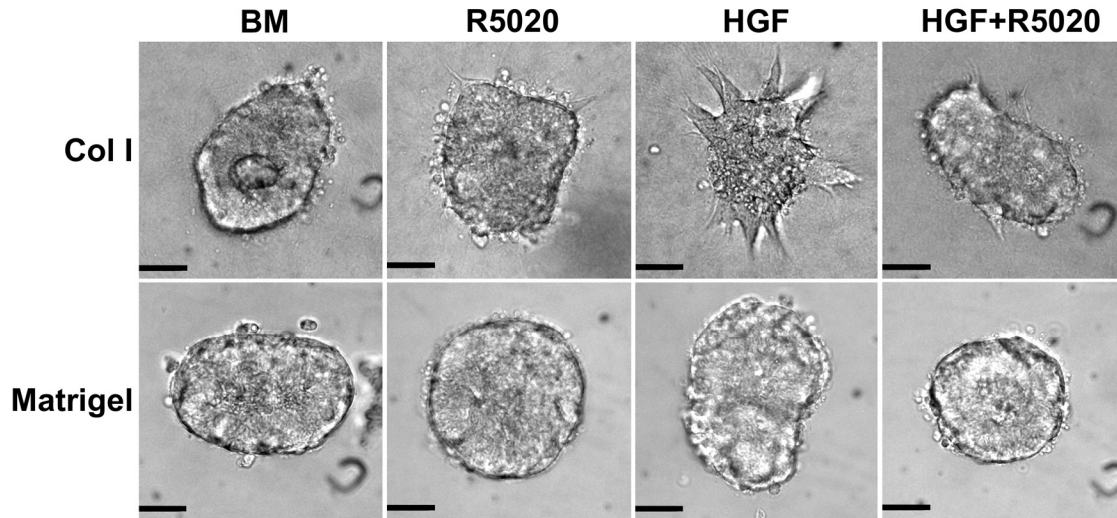


R5020 reduces HGF-induced tubulogenesis.

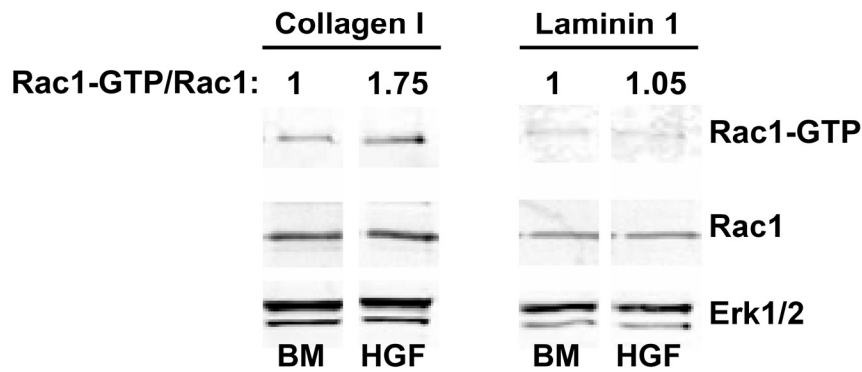
Organoids were treated with BM, HGF or HGF+R5020 for 24h. A). Representative phase contrast micrographs of organoids at 4 and 24h. White arrowheads indicate extensions, white arrows indicate chains and black arrowheads indicate tubules. Scale bar = 0.05mm. B). Quantitation of extensions, chains and tubules after 4 and 24h treatment. a,b, $p < 0.05$ that HGF+R5020 reduced the numbers of indicated structures compared to HGF ($n=7$). C). The effect of R5020 on HGF-induced Rac1 activation. Rac1-GTP levels at 4h were determined by Rac1-GTP pull down and immunoblot. For densitometry, Rac1-GTP was normalized to total Rac1 and fold change relative to BM was calculated. * $p < 0.05$ HGF Rac1-GTP greater than BM Rac1-GTP. # $p < 0.05$ R5020 reduced HGF Rac1-GTP ($n = 3$). D). Representative immunoblots of the R5020 effect on phospho-Src, phospho-FAK, phospho-Erk, and phospho-AKT 4h after treatment.

FIGURE 11

A



B

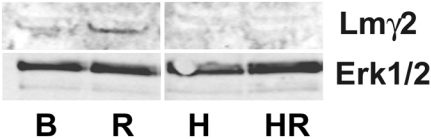


Laminin reduces HGF-induced tubulogenesis.

Organoids were cultured as 3D culture in collagen I (Col I) or Matrigel and treated with BM, HGF, R5020 or HGF+R5020 for 24h. A). Representative phase contrast micrographs of organoids after 24h treatment. Note the absence of tubules in Matrigel +HGF culture. Scale bar = 0.05mm. B). Culture on laminin-1 reduces HGF-induced Rac1 activity. Organoids were cultured as monolayer on Col I or laminin-1 and treated with BM or HGF for 4h. Rac1-GTP levels were analyzed by Rac1-GTP pull down and immunoblot. For densitometry, Rac1-GTP was normalized to total Rac1 and fold change relative to BM was calculated.

FIGURE 12

A



B

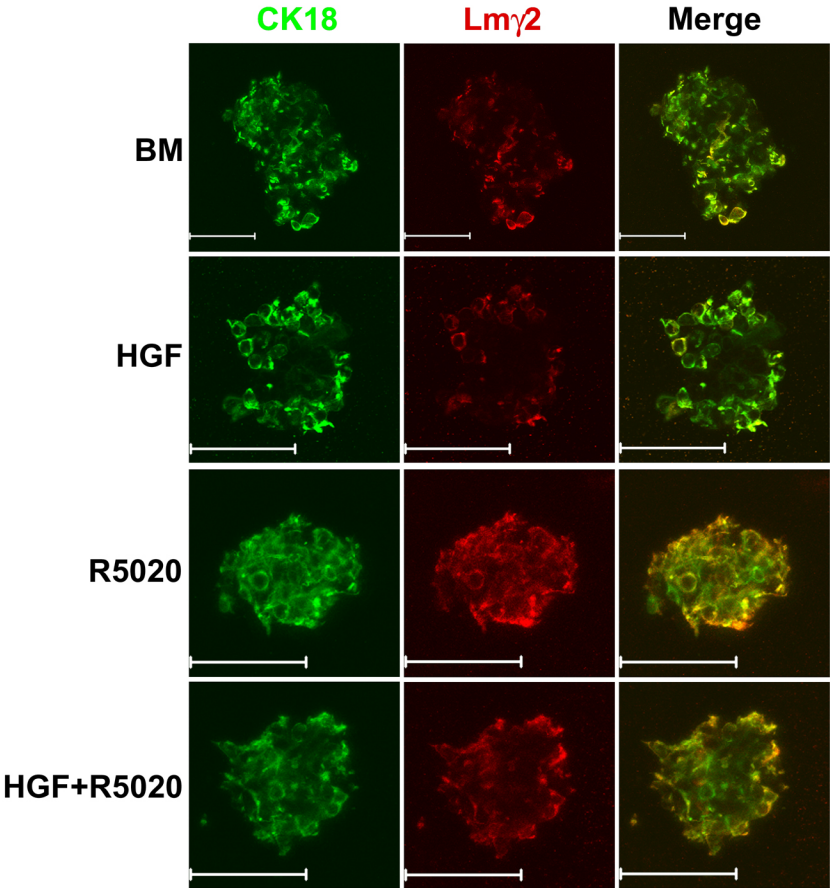
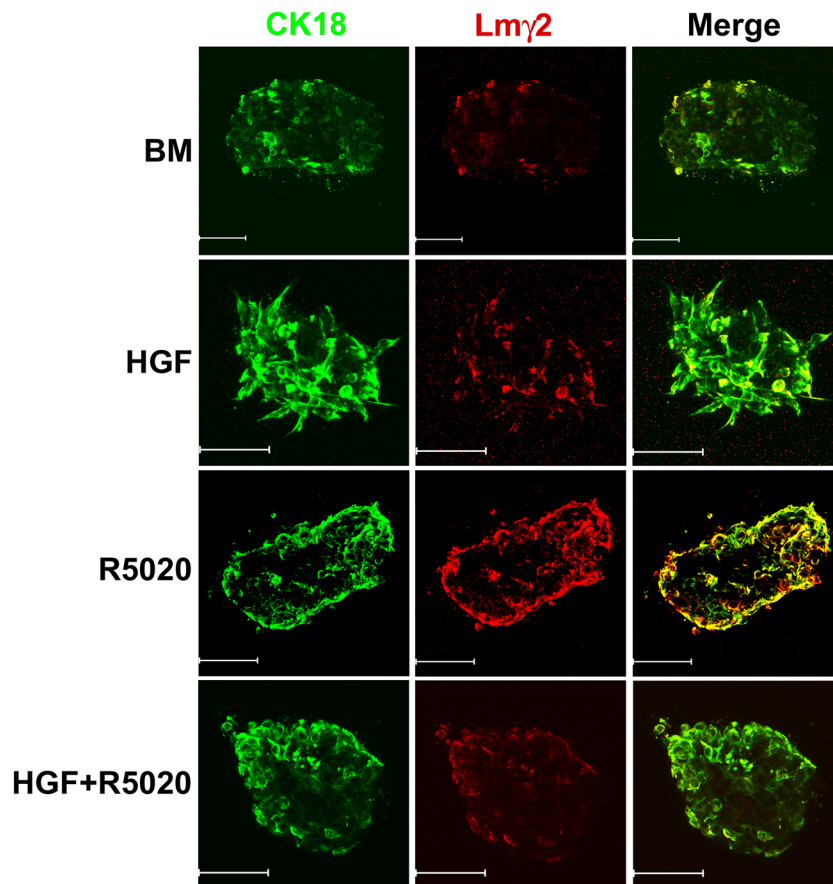


FIGURE 12 (cont'd)

C

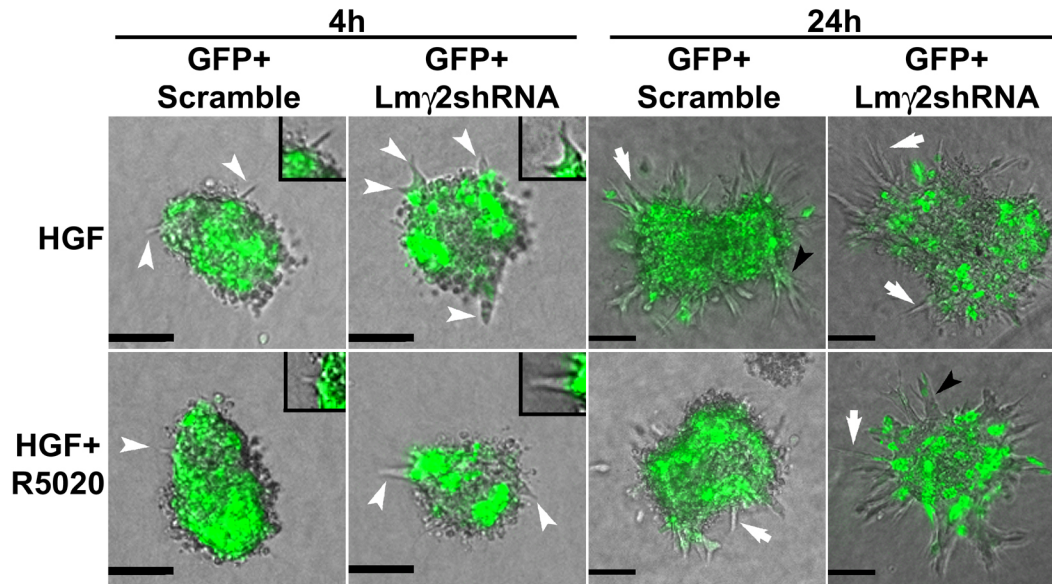


R5020 induces Laminin- γ 2 expression in mammary organoids.

Organoids cultured in collagen I were treated with BM (B), HGF (H), R5020 (R) or HGF+R5020 (HR) for 4h or 24h. A). Immunoblot analysis of laminin- γ 2 (Lm γ 2) after 4h treatment. (n = 2) B,C). Confocal immunofluorescence images of organoids at 4h (B) or 24h (C) after in situ double antibody labeling with anti-CK-18 (green) and anti- Lm γ 2 (red). Note increased intensity of Lm γ 2 (red) staining in R5020- and HGF+R5020-treated organoids. Scale bar = 0.05mm. (n = 1).

FIGURE 13

A



B

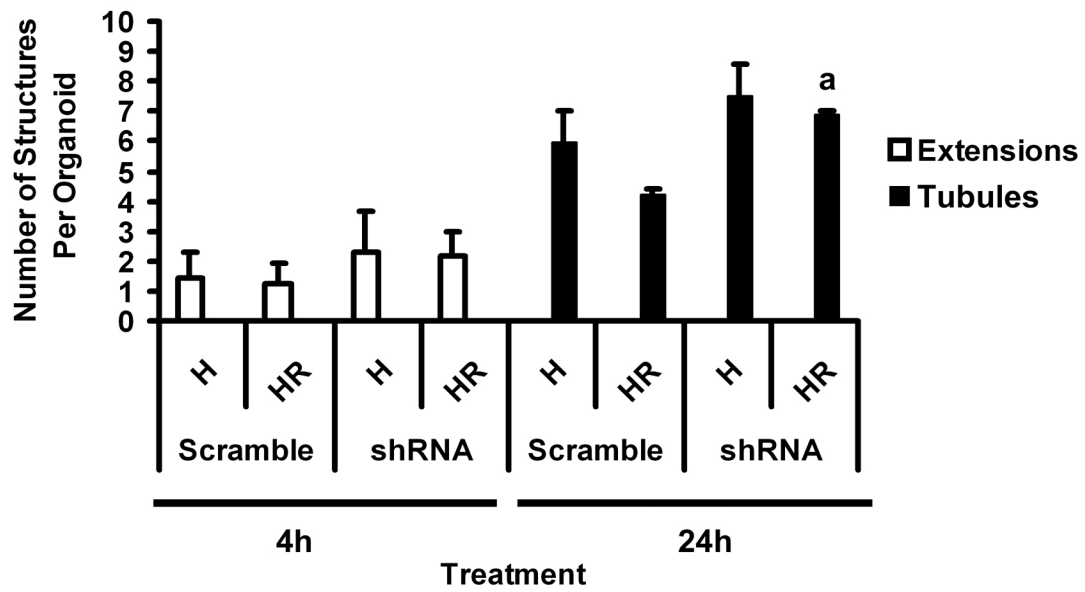
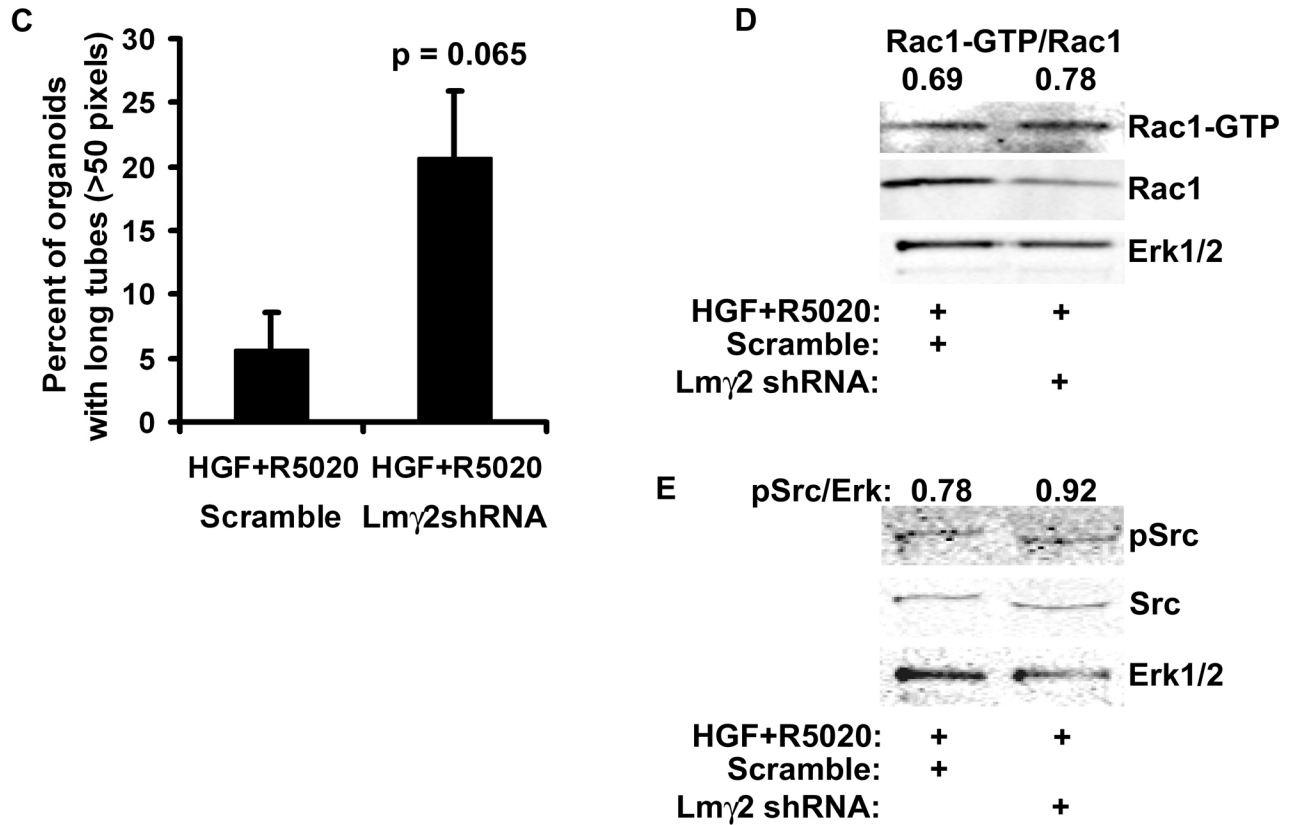


FIGURE 13 (cont'd)

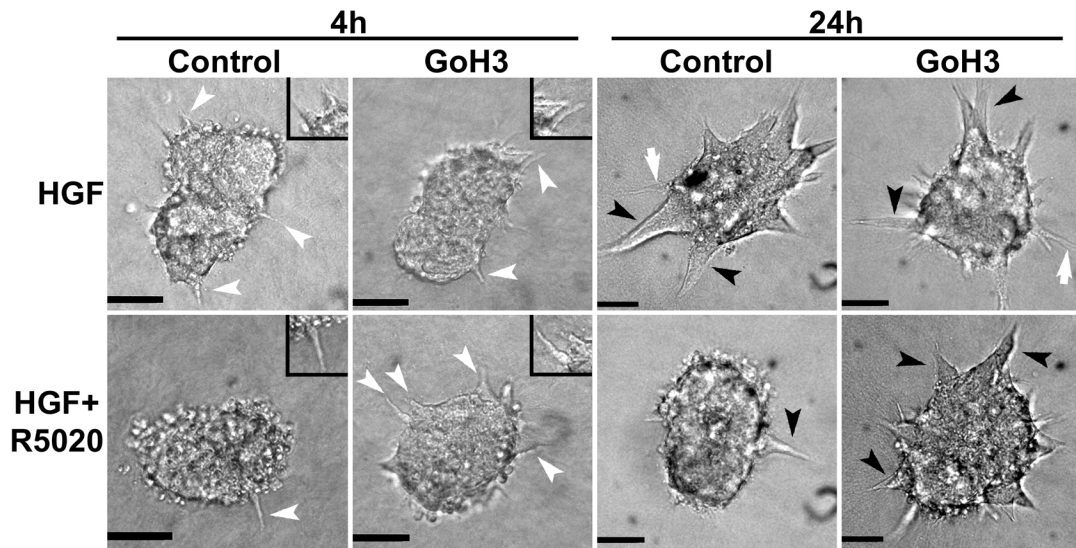


Laminin- γ 2 shRNA reverses the effect of R5020 on tubulogenesis.

Organoids were infected with control virus (GFP+ Scramble) or virus carrying shRNA against Laminin- γ 2 (GFP+ Lm γ 2shRNA). 24h post infection, organoids were treated with HGF (H) or HGF+R5020 (HR) for 24h. A). Representative phase contrast and GFP overlay images of organoids at 4 and 24h. White arrowheads indicate extensions, white arrows indicate chains and black arrowheads indicate tubules; insets are enlargements of GFP+ and GFP- extensions. B). Quantitation of extensions, chains and tubules at 4 or 24h. a, $p < 0.05$ that Lm γ 2shRNA increased the number of tubules compared to HR controls. 48-67 organoids were analyzed per treatment from two separate experiments. C). Quantitation of the percent of organoids producing long tubules (≥ 50 pixels). 134-141 organoids were analyzed per treatment from 3 separate experiments. The effect of Lm γ 2shRNA on Rac1 activation (D) and phospho-Src (E). Rac1-GTP levels were analyzed by Rac1-GTP pull down and immunoblot. For densitometry, Rac1-GTP was normalized to total Rac1. Phospho-Src was assessed by immunoblot 4h after treatment with HGF+R5020.

FIGURE 14

A



B

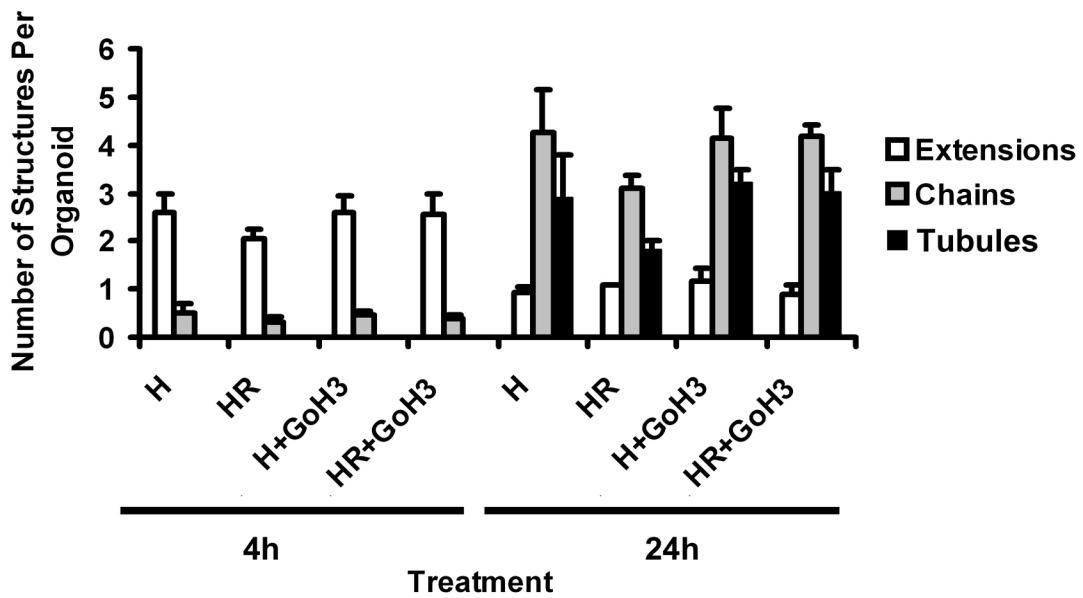
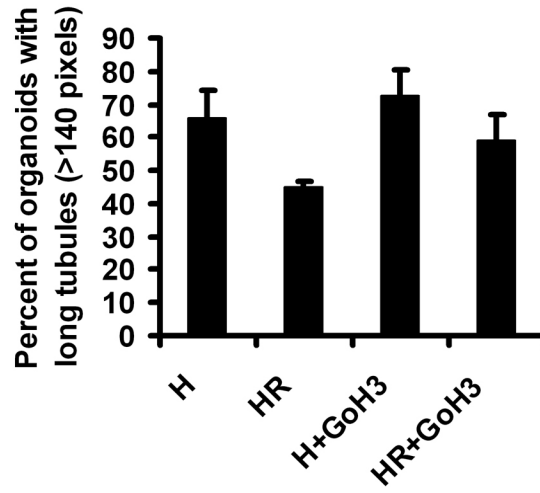
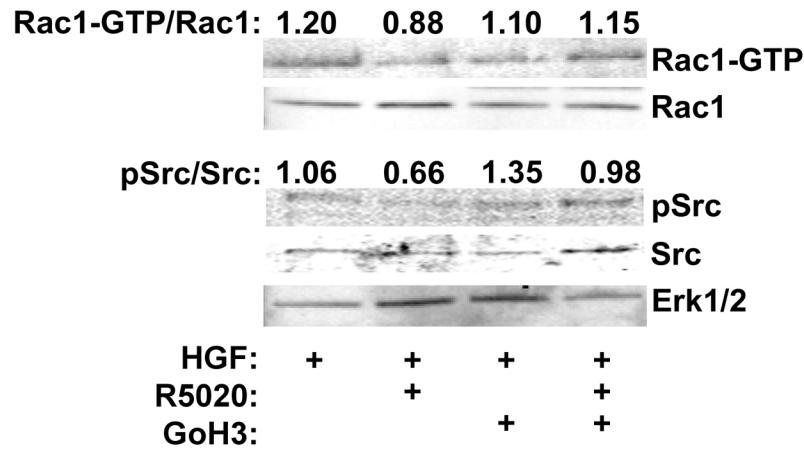


FIGURE 14 (cont'd)

C



D



Effect of antibody blocking of $\alpha 6$ -integrin R5020 inhibition of tubulogenesis. Organoids were treated with HGF (H) or HGF+R5020 (HR) in the presence or absence of the $\alpha 6$ -integrin function-blocking antibody, GoH3 (10 $\mu\text{g}/\text{ml}$) for 24h. A). Representative phase contrast micrographs of organoids at 4 and 24h. White arrowheads indicate extensions, white arrows indicate chains and black arrowheads indicate tubules; inset are enlargement of extensions. Scale bar = 0.05mm. B). Quantitation of extensions, chains and tubules after 4 and 24h treatment with the $\alpha 6$ -integrin blocking antibody. 54-69 organoids were analyzed per treatment from 2 separate experiments. C). Percent of organoids forming long tubules (≥ 140 pixels) after 24h treatment. D). The effect of $\alpha 6$ -integrin blocking antibody on Rac1 activity. Representative experiment showing Rac1-GTP levels at 4h analyzed by Rac1-GTP pull down and immunoblot. For densitometry, Rac1-GTP was normalized to total Rac1.

FIGURE 15

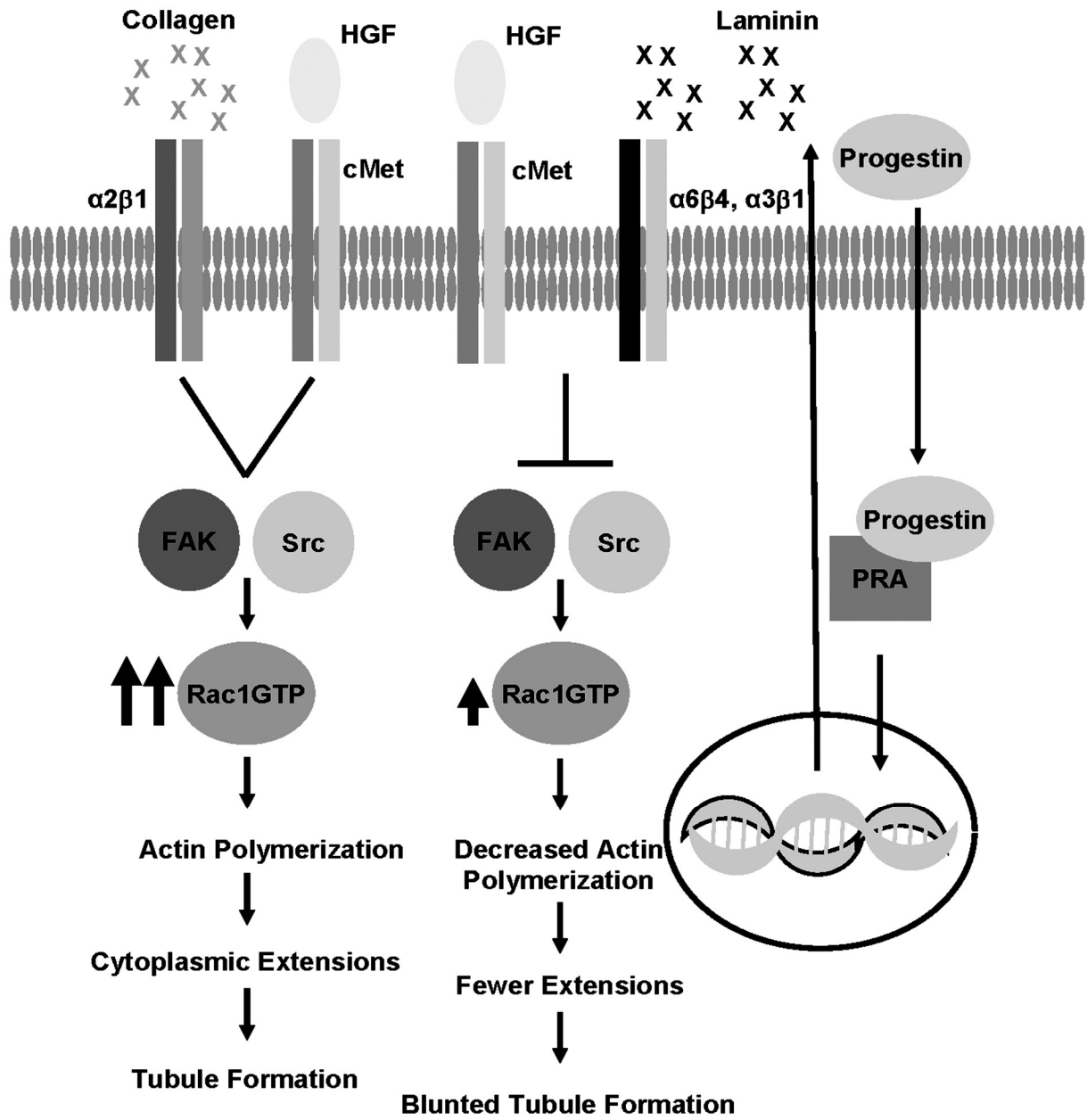


FIGURE 15 (cont'd)

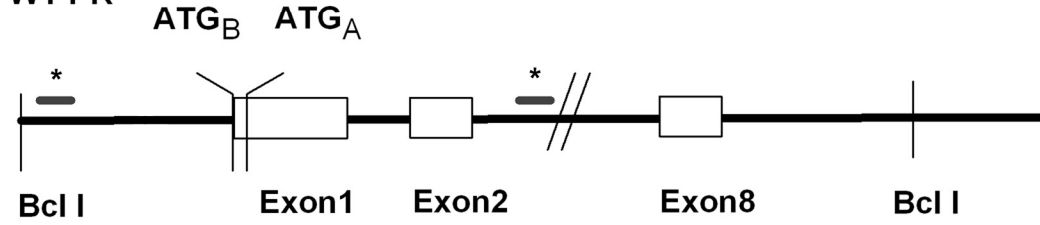
Proposed mechanism for R5020-blunted tubulogenesis.

In the presence of collagen I, collagen I/ $\alpha_2\beta_1$ -integrin and HGF/cMet signaling increase levels of phosphorylated Src, FAK and levels of Rac1-GTP to initiate the formation of extensions promoting tubulogenesis of organoids. In the presence of HGF+R5020, R5020 signaling through PRA induces LM-5 expression changing the ECM composition. The combination of laminin/ α_6 -integrin and HGF/cMet signaling results in decreased levels of phosphorylated Src, FAK and levels of Rac1-GTP inhibiting extension formation and blunting tubulogenesis.

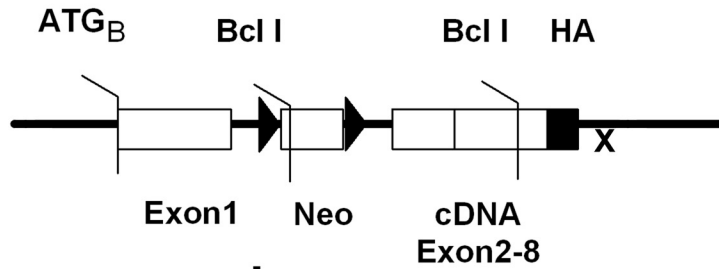
FIGURE 16

A

WT PR



PRAKO
Targeting Vector



PRAKO

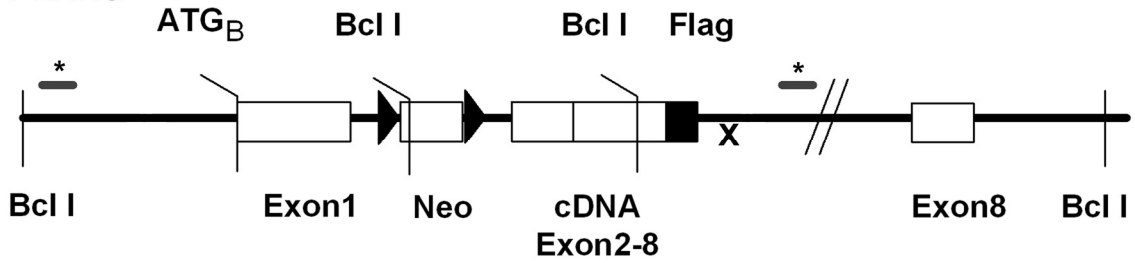
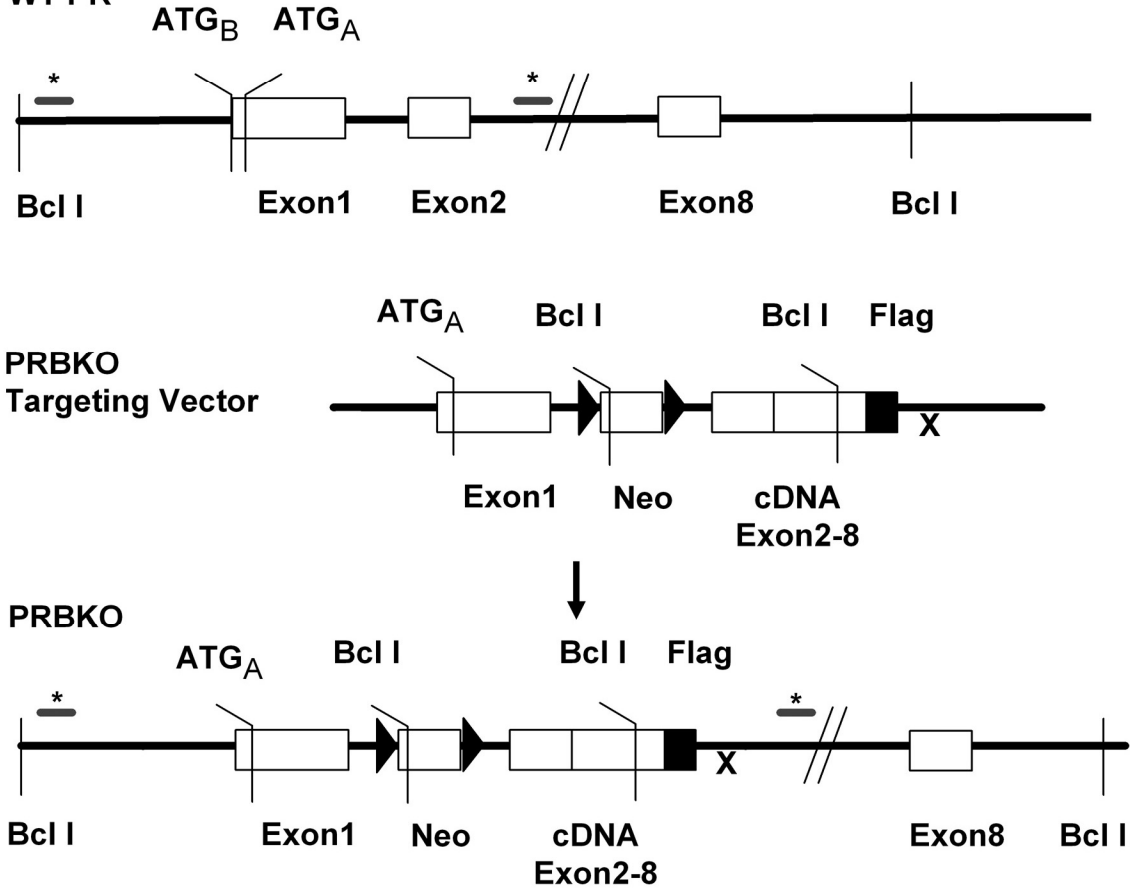


FIGURE 16 (cont'd)

B WT PR



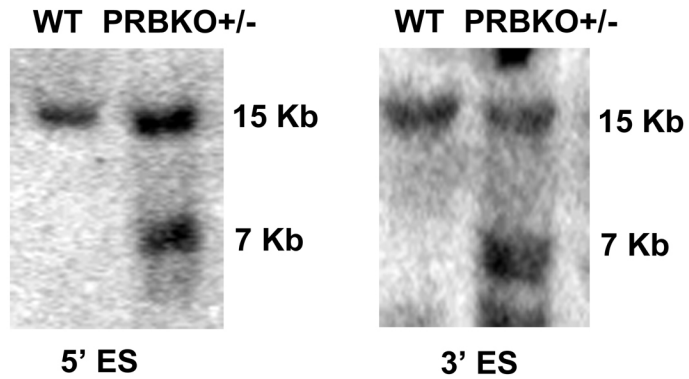
Strategy for developing PRA and PRB knockout Balb/c mice.

A). Diagram shows the gene-targeting strategy for developing the PRAKO allele.

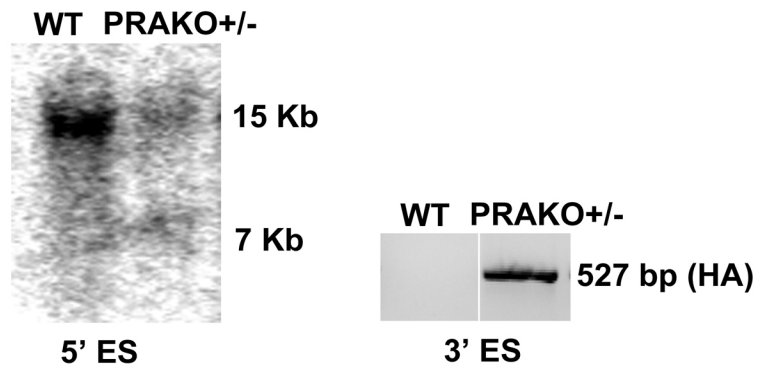
Wild type (WT) PR locus contains both PRA and PRB ATG sites. For simplicity, exons 3-7 were not drawn, as indicated by double hash marks. The PR locus is flanked by Bcl I restriction sites approximately 15 Kb apart. Asterisks indicate position of 5' and 3' DNA probes used for Southern blot analysis. The PRAKO targeting vector contains a 5.5 Kb 5' and a 5 Kb 3' recombination arms that were generated from Balb/C DNA. Only the PRB ATG site was present in the targeting vector. Neomycin selection cassette (Neo) was included in intron 1. The cassette was flanked with loxP sites (triangles). Endogenous PR exon 2 was fused to cDNA encoding exons 3-8 that contained an HA epitope tag. An SV40 polyadenylation sequence was placed after the cDNA in the 3' recombination arm. The targeting vector introduces two novel Bcl I sites, within Neo and the cDNA. Homologous recombination with the targeting vector results in the PRAKO allele. B.) The gene-targeting strategy for the PRBKO strategy. A similar approach to generating the PRAKO allele was used. Only the PRA ATG site was present in the targeting vector. The cDNA contained a Flag epitope tag.

FIGURE 17

A



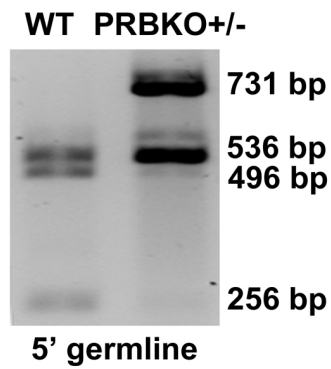
B



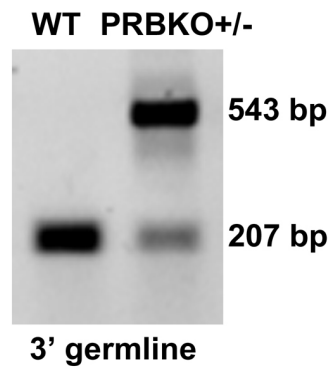
Identification of PRBKO and PRAKO alleles in ES cells. ES cell DNA was digested with Bcl I to analyze the 5' and 3' ends by Southern blot. A). Recombination of the 5' and 3' ends for the PRBKO allele. B). Recombination of the 5' end and verified presence of the HA tag for the PRAKO allele.

FIGURE 18

A



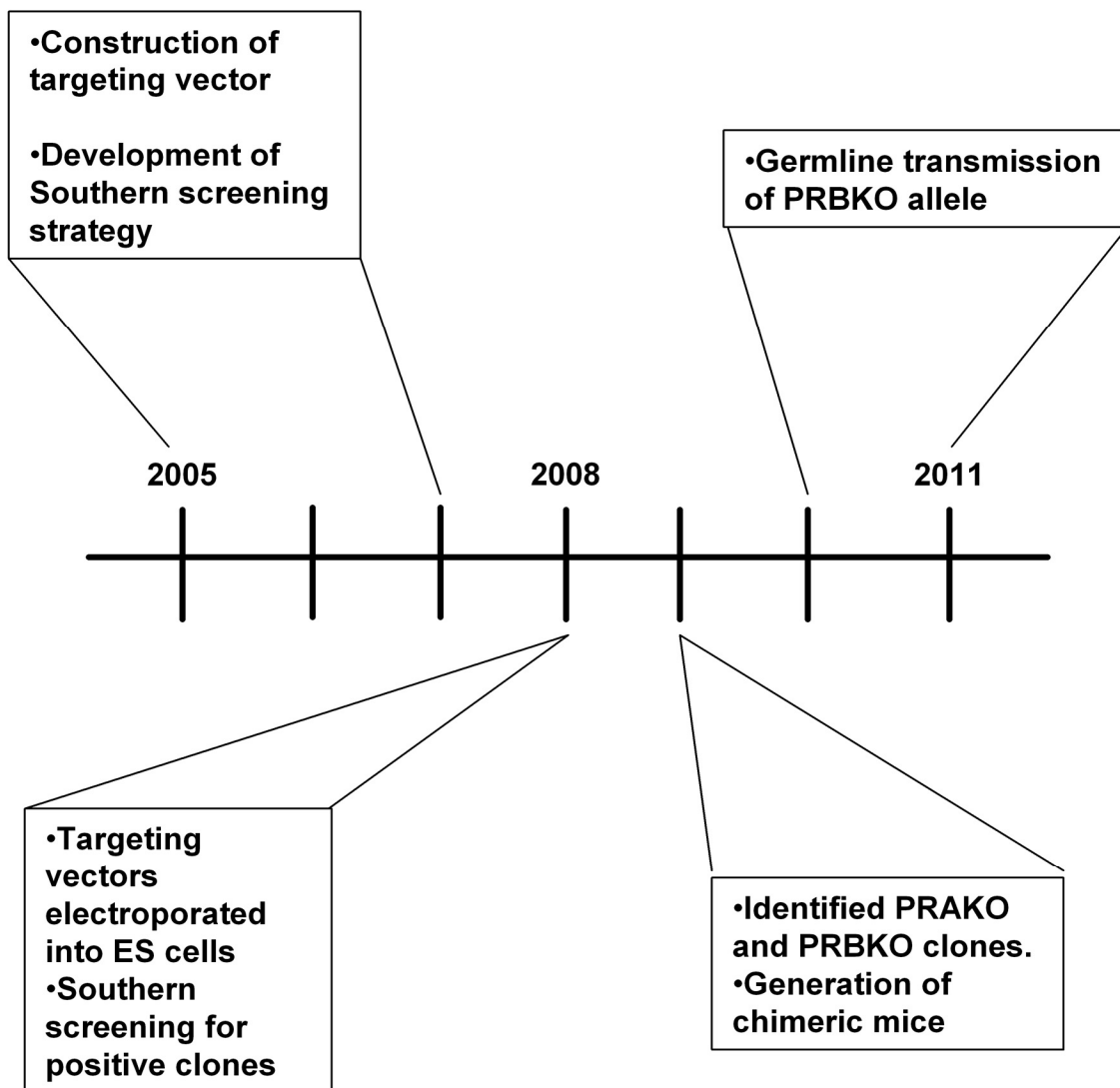
B



Identification of germline PRBKO allele.

A). 5' germline transmission of the PRBKO allele. Primers were designed flanking the ATG site. The PCR product was then digested with Bsp HI. The mutation within the PRBKO allele eliminates a Bsp HI site. B). 3' germline transmission of the PRBKO allele. Primers were designed within intron 2 that flank the insertion site of the SV40 polyadenylation sequence. The SV40 sequence increases the size of the PCR product.

FIGURE 19



Timeline for generating Balb/c PRA and PRB knockout mice.

Infection	Treatment	Fold Change
Scramble	HGF	1
	HGF+R5020	1.2
Lm γ 2 shRNA	HGF	-3.14
	HGF+R5020	-2.6

TABLE 1. Quantitative RT-PCR analysis of fold change of Laminin- γ 2 mRNA after knockdown with Lm γ 2 shRNA.

REFERENCES

REFERENCES

1. **Cunha GR, Young P, Hom YK, Cooke PS, Taylor JA, Lubahn DB** 1997 Elucidation of a role for stromal steroid hormone receptors in mammary gland growth and development using tissue recombinants. *Journal of mammary gland biology and neoplasia* 2:393-402
2. **Mallepell S, Krust A, Chambon P, Briskin C** 2006 Paracrine signaling through the epithelial estrogen receptor alpha is required for proliferation and morphogenesis in the mammary gland. *Proceedings of the National Academy of Sciences of the United States of America* 103:2196-2201
3. **Zhang HZ, Bennett JM, Smith KT, Sunil N, Haslam SZ** 2002 Estrogen mediates mammary epithelial cell proliferation in serum-free culture indirectly via mammary stroma-derived hepatocyte growth factor. *Endocrinology* 143:3427-3434
4. **Bascom JL, Fata JE, Hirai Y, Sternlicht MD, Bissell MJ** 2005 Epimorphin overexpression in the mouse mammary gland promotes alveolar hyperplasia and mammary adenocarcinoma. *Cancer research* 65:8617-8621
5. **Garner OB, Bush KT, Nigam KB, Yamaguchi Y, Xu D, Esko JD, Nigam SK** Stage-dependent regulation of mammary ductal branching by heparan sulfate and HGF-cMet signaling. *Dev Biol* 355:394-403
6. **Ciarloni L, Mallepell S, Briskin C** 2007 Amphiregulin is an essential mediator of estrogen receptor alpha function in mammary gland development. *Proceedings of the National Academy of Sciences of the United States of America* 104:5455-5460
7. **Wiesen JF, Young P, Werb Z, Cunha GR** 1999 Signaling through the stromal epidermal growth factor receptor is necessary for mammary ductal development. *Development (Cambridge, England)* 126:335-344
8. **Mulac-Jericevic B, Lydon JP, DeMayo FJ, Conneely OM** 2003 Defective mammary gland morphogenesis in mice lacking the progesterone receptor B isoform. *Proceedings of the National Academy of Sciences of the United States of America* 100:9744-9749
9. **Soriano JV, Pepper MS, Nakamura T, Orci L, Montesano R** 1995 Hepatocyte growth factor stimulates extensive development of branching duct-like structures by cloned mammary gland epithelial cells. *J Cell Sci* 108 (Pt 2):413-430
10. **Sunil N, Bennett JM, Haslam SZ** 2002 Hepatocyte growth factor is required for progestin-induced epithelial cell proliferation and alveolar-like morphogenesis in serum-free culture of normal mammary epithelial cells. *Endocrinology* 143:2953-2960

11. **Haslam SZ, Drolet A, Smith K, Tan M, Aupperlee M** 2008 Progesterin-regulated luminal cell and myoepithelial cell-specific responses in mammary organoid culture. *Endocrinology* 149:2098-2107
12. **Richert MM, Schwertfeger KL, Ryder JW, Anderson SM** 2000 An atlas of mouse mammary gland development. *Journal of mammary gland biology and neoplasia* 5:227-241
13. **Haslam SZ, Nummy KA** 1992 The ontogeny and cellular distribution of estrogen receptors in normal mouse mammary gland. *The Journal of steroid biochemistry and molecular biology* 42:589-595
14. **Aupperlee MD, Smith KT, Kariagina A, Haslam SZ** 2005 Progesterone Receptor Isoforms A and B: Temporal and Spatial Differences in Expression During Murine Mammary Gland Development. *Endocrinology* 146:3577-3588.
15. **Zeps N, Bentel JM, Papadimitriou JM, Dawkins HJ** 1999 Murine progesterone receptor expression in proliferating mammary epithelial cells during normal pubertal development and adult estrous cycle. Association with α and β status. *J Histochem Cytochem* 47:1323-1330
16. **Beleut M, Rajaram RD, Caikovski M, Ayyanan A, Germano D, Choi Y, Schneider P, Briskin C** Two distinct mechanisms underlie progesterone-induced proliferation in the mammary gland. *Proceedings of the National Academy of Sciences of the United States of America* 107:2989-2994
17. **Katz E, Streuli CH** 2007 The extracellular matrix as an adhesion checkpoint for mammary epithelial function. *Int J Biochem Cell Biol* 39:715-726
18. **Keely PJ, Wu JE, Santoro SA** 1995 The spatial and temporal expression of the $\alpha 2$ $\beta 1$ integrin and its ligands, collagen I, collagen IV, and laminin, suggest important roles in mouse mammary morphogenesis. *Differentiation; research in biological diversity* 59:1-13
19. **Woodward TL, Mienaltowski AS, Modi RR, Bennett JM, Haslam SZ** 2001 Fibronectin and the $\alpha(5)\beta(1)$ integrin are under developmental and ovarian steroid regulation in the normal mouse mammary gland. *Endocrinology* 142:3214-3222
20. **Nelson CM, Bissell MJ** 2006 Of extracellular matrix, scaffolds, and signaling: tissue architecture regulates development, homeostasis, and cancer. *Annu Rev Cell Dev Biol* 22:287-309
21. **Xie J, Haslam SZ** 1997 Extracellular matrix regulates ovarian hormone-dependent proliferation of mouse mammary epithelial cells. *Endocrinology* 138:2466-2473
22. **Sternlicht MD** 2006 Key stages in mammary gland development: the cues that regulate ductal branching morphogenesis. *Breast Cancer Res* 8:201

23. **Haslam SZ** 1989 The ontogeny of mouse mammary gland responsiveness to ovarian steroid hormones. *Endocrinology* 125:2766-2772
24. **Coleman S, Silberstein GB, Daniel CW** 1988 Ductal morphogenesis in the mouse mammary gland: evidence supporting a role for epidermal growth factor. *Dev Biol* 127:304-315
25. **Kenney NJ, Bowman A, Korach KS, Barrett JC, Salomon DS** 2003 Effect of exogenous epidermal-like growth factors on mammary gland development and differentiation in the estrogen receptor-alpha knockout (ERKO) mouse. *Breast cancer research and treatment* 79:161-173
26. **Coleman-Krnacik S, Rosen JM** 1994 Differential temporal and spatial gene expression of fibroblast growth factor family members during mouse mammary gland development. *Mol Endocrinol* 8:218-229
27. **Lu P, Ewald AJ, Martin GR, Werb Z** 2008 Genetic mosaic analysis reveals FGF receptor 2 function in terminal end buds during mammary gland branching morphogenesis. *Dev Biol* 321:77-87
28. **Kamalati T, Niranjana B, Yant J, Buluwela L** 1999 HGF/SF in mammary epithelial growth and morphogenesis: in vitro and in vivo models. *Journal of mammary gland biology and neoplasia* 4:69-77
29. **Benvenuti S, Comoglio PM** 2007 The MET receptor tyrosine kinase in invasion and metastasis. *Journal of cellular physiology* 213:316-325
30. **Takayama H, LaRochelle WJ, Sharp R, Otsuka T, Kriebel P, Anver M, Aaronson SA, Merlino G** 1997 Diverse tumorigenesis associated with aberrant development in mice overexpressing hepatocyte growth factor/scatter factor. *Proceedings of the National Academy of Sciences of the United States of America* 94:701-706
31. **Yant J, Buluwela L, Niranjana B, Gusterson B, Kamalati T** 1998 In vivo effects of hepatocyte growth factor/scatter factor on mouse mammary gland development. *Experimental cell research* 241:476-481
32. **Rosario M, Birchmeier W** 2003 How to make tubes: signaling by the Met receptor tyrosine kinase. *Trends in cell biology* 13:328-335
33. **Niranjana B, Buluwela L, Yant J, Perusinghe N, Atherton A, Phippard D, Dale T, Gusterson B, Kamalati T** 1995 HGF/SF: a potent cytokine for mammary growth, morphogenesis and development. *Development (Cambridge, England)* 121:2897-2908
34. **Fendrick JL, Raafat AM, Haslam SZ** 1998 Mammary gland growth and development from the postnatal period to postmenopause: ovarian steroid receptor ontogeny and regulation in the mouse. *Journal of mammary gland biology and neoplasia* 3:7-22

35. **Shyamala G, Chou YC, Louie SG, Guzman RC, Smith GH, Nandi S** 2002 Cellular expression of estrogen and progesterone receptors in mammary glands: regulation by hormones, development and aging. *The Journal of steroid biochemistry and molecular biology* 80:137-148.
36. **Saji S, Jensen EV, Nilsson S, Rylander T, Warner M, Gustafsson JA** 2000 Estrogen receptors alpha and beta in the rodent mammary gland. *Proceedings of the National Academy of Sciences of the United States of America* 97:337-342
37. **Kastner P, Krust A, Turcotte B, Stropp U, Tora L, Gronemeyer H, Chambon P** 1990 Two distinct estrogen-regulated promoters generate transcripts encoding the two functionally different human progesterone receptor forms A and B. *Embo J* 9:1603-1614
38. **Kraus WL, Montano MM, Katzenellenbogen BS** 1993 Cloning of the rat progesterone receptor gene 5'-region and identification of two functionally distinct promoters. *Mol Endocrinol* 7:1603-1616
39. **Conneely OM, Kettelberger DM, Tsai MJ, Schrader WT, O'Malley BW** 1989 The chicken progesterone receptor A and B isoforms are products of an alternate translation initiation event. *The Journal of biological chemistry* 264:14062-14064.
40. **Leonhardt SA, Boonyaratanakornkit V, Edwards DP** 2003 Progesterone receptor transcription and non-transcription signaling mechanisms. *Steroids* 68:761-770
41. **Sartorius CA, Melville MY, Hovland AR, Tung L, Takimoto GS, Horwitz KB** 1994 A third transactivation function (AF3) of human progesterone receptors located in the unique N-terminal segment of the B-isoform. *Mol Endocrinol* 8:1347-1360.
42. **Tung L, Abdel-Hafiz H, Shen T, Harvell DM, Nitao LK, Richer JK, Sartorius CA, Takimoto GS, Horwitz KB** 2006 Progesterone receptors (PR)-B and -A regulate transcription by different mechanisms: AF-3 exerts regulatory control over coactivator binding to PR-B. *Mol Endocrinol* 20:2656-2670
43. **Hovland AR, Powell RL, Takimoto GS, Tung L, Horwitz KB** 1998 An N-terminal inhibitory function, IF, suppresses transcription by the A-isoform but not the B-isoform of human progesterone receptors. *The Journal of biological chemistry* 273:5455-5460.
44. **Boonyaratanakornkit V, Edwards DP** 2004 Receptor mechanisms of rapid extranuclear signalling initiated by steroid hormones. *Essays Biochem* 40:105-120
45. **Boonyaratanakornkit V, McGowan E, Sherman L, Mancini MA, Cheskis BJ, Edwards DP** 2007 The role of extranuclear signaling actions of progesterone receptor in mediating progesterone regulation of gene expression and the cell cycle. *Mol Endocrinol* 21:359-375

46. **Lange CA** 2008 Integration of progesterone receptor action with rapid signaling events in breast cancer models. *The Journal of steroid biochemistry and molecular biology* 108:203-212
47. **Mulac-Jericevic B, Mullinax RA, DeMayo FJ, Lydon JP, Conneely OM** 2000 Subgroup of reproductive functions of progesterone mediated by progesterone receptor-B isoform. *Science* 289:1751-1754.
48. **Aupperlee MD, Drolet AA, Durairaj S, Wang W, Schwartz RC, Haslam SZ** 2009 Strain-specific differences in the mechanisms of progesterone regulation of murine mammary gland development. *Endocrinology* 150:1485-1494
49. **Aupperlee MD, Haslam SZ** 2007 Differential hormonal regulation and function of PR isoforms in normal adult mouse mammary gland. *Endocrinology*
50. **Montesano R, Matsumoto K, Nakamura T, Orci L** 1991 Identification of a fibroblast-derived epithelial morphogen as hepatocyte growth factor. *Cell* 67:901-908
51. **Itakura A, Kurauchi O, Morikawa S, Okamura M, Furugori K, Mizutani S** 1997 Involvement of hepatocyte growth factor in formation of bronchoalveolar structures in embryonic rat lung in primary culture. *Biochemical and biophysical research communications* 241:98-103
52. **Furue M, Okamoto T, Hayashi H, Sato JD, Asashima M, Saito S** 1999 Effects of hepatocyte growth factor (HGF) and activin A on the morphogenesis of rat submandibular gland-derived epithelial cells in serum-free collagen gel culture. *In Vitro Cell Dev Biol Anim* 35:131-135
53. **Pollack AL, Runyan RB, Mostov KE** 1998 Morphogenetic mechanisms of epithelial tubulogenesis: MDCK cell polarity is transiently rearranged without loss of cell-cell contact during scatter factor/hepatocyte growth factor-induced tubulogenesis. *Dev Biol* 204:64-79
54. **O'Brien LE, Tang K, Kats ES, Schutz-Geschwender A, Lipschutz JH, Mostov KE** 2004 ERK and MMPs sequentially regulate distinct stages of epithelial tubule development. *Developmental cell* 7:21-32
55. **Ridley AJ, Hall A** 1992 The small GTP-binding protein rho regulates the assembly of focal adhesions and actin stress fibers in response to growth factors. *Cell* 70:389-399
56. **Ridley AJ, Comoglio PM, Hall A** 1995 Regulation of scatter factor/hepatocyte growth factor responses by Ras, Rac, and Rho in MDCK cells. *Mol Cell Biol* 15:1110-1122
57. **Rogers KK, Jou TS, Guo W, Lipschutz JH** 2003 The Rho family of small GTPases is involved in epithelial cystogenesis and tubulogenesis. *Kidney Int* 63:1632-1644

58. **Ishibe S, Joly D, Liu ZX, Cantley LG** 2004 Paxillin serves as an ERK-regulated scaffold for coordinating FAK and Rac activation in epithelial morphogenesis. *Mol Cell* 16:257-267
59. **Tushir JS, D'Souza-Schorey C** 2007 ARF6-dependent activation of ERK and Rac1 modulates epithelial tubule development. *Embo J* 26:1806-1819
60. **Yu W, O'Brien LE, Wang F, Bourne H, Mostov KE, Zegers MM** 2003 Hepatocyte growth factor switches orientation of polarity and mode of movement during morphogenesis of multicellular epithelial structures. *Mol Biol Cell* 14:748-763
61. **Khwaja A, Lehmann K, Marte BM, Downward J** 1998 Phosphoinositide 3-kinase induces scattering and tubulogenesis in epithelial cells through a novel pathway. *The Journal of biological chemistry* 273:18793-18801
62. **Rahimi N, Hung W, Tremblay E, Saulnier R, Elliott B** 1998 c-Src kinase activity is required for hepatocyte growth factor-induced motility and anchorage-independent growth of mammary carcinoma cells. *The Journal of biological chemistry* 273:33714-33721
63. **Chianale F, Rainero E, Cianflone C, Bettio V, Pighini A, Porporato PE, Filigheddu N, Serini G, Sinigaglia F, Baldanzi G, Graziani A** Diacylglycerol kinase alpha mediates HGF-induced Rac activation and membrane ruffling by regulating atypical PKC and RhoGDI. *Proceedings of the National Academy of Sciences of the United States of America* 107:4182-4187
64. **Luo J, Deng ZL, Luo X, Tang N, Song WX, Chen J, Sharff KA, Luu HH, Haydon RC, Kinzler KW, Vogelstein B, He TC** 2007 A protocol for rapid generation of recombinant adenoviruses using the AdEasy system. *Nat Protoc* 2:1236-1247
65. **Santos SJ, Aupperlee MD, Xie J, Durairaj S, Miksicek R, Conrad SE, Leipprandt JR, Tan YS, Schwartz RC, Haslam SZ** 2009 Progesterone receptor A-regulated gene expression in mammary organoid cultures. *The Journal of steroid biochemistry and molecular biology* 115:161-172
66. **Chianale F, Cutrupi S, Rainero E, Baldanzi G, Porporato PE, Traini S, Filigheddu N, Gnocchi VF, Santoro MM, Parolini O, van Blitterswijk WJ, Sinigaglia F, Graziani A** 2007 Diacylglycerol kinase-alpha mediates hepatocyte growth factor-induced epithelial cell scatter by regulating Rac activation and membrane ruffling. *Mol Biol Cell* 18:4859-4871
67. **Santos OF, Nigam SK** 1993 HGF-induced tubulogenesis and branching of epithelial cells is modulated by extracellular matrix and TGF-beta. *Dev Biol* 160:293-302
68. **Williams MJ, Clark P** 2003 Microscopic analysis of the cellular events during scatter factor/hepatocyte growth factor-induced epithelial tubulogenesis. *J Anat* 203:483-503

69. **Xie JW, Haslam SZ** 2008 Extracellular matrix, Rac1 signaling, and estrogen-induced proliferation in MCF-7 breast cancer cells. *Breast cancer research and treatment* 110:257-268
70. **Chen HC, Chan PC, Tang MJ, Cheng CH, Chang TJ** 1998 Tyrosine phosphorylation of focal adhesion kinase stimulated by hepatocyte growth factor leads to mitogen-activated protein kinase activation. *The Journal of biological chemistry* 273:25777-25782
71. **Popsueva A, Poteryaev D, Arighi E, Meng X, Angers-Loustau A, Kaplan D, Saarma M, Sariola H** 2003 GDNF promotes tubulogenesis of GFRalpha1-expressing MDCK cells by Src-mediated phosphorylation of Met receptor tyrosine kinase. *The Journal of cell biology* 161:119-129
72. **Boonyaratanakornkit V, Scott MP, Ribon V, Sherman L, Anderson SM, Maller JL, Miller WT, Edwards DP** 2001 Progesterone receptor contains a proline-rich motif that directly interacts with SH3 domains and activates c-Src family tyrosine kinases. *Mol Cell* 8:269-280.
73. **Montero Girard G, Vanzulli SI, Cerliani JP, Bottino MC, Bolado J, Vela J, Becu-Villalobos D, Benavides F, Gutkind S, Patel V, Molinolo A, Lanari C** 2007 Association of estrogen receptor-alpha and progesterone receptor A expression with hormonal mammary carcinogenesis: role of the host microenvironment. *Breast Cancer Res* 9:R22